Quaternary Science Reviews 363 (2025) 109443

Contents lists available at ScienceDirect

Quaternary Science Reviews

journal homepage: www.elsevier.com/locate/quascirev

A 2000-year record of hydroclimate variability inferred from oxygen isotopes in lake sediments on Kangaroo Island (Karti/Karta), South Australia

Mahfuzur Rahman[a,b,*], Lucinda Duxbury[a,c], Haidee Cadd[d], Robert Klaebe[a,e], Geraldine Jacobsen[f], John Tibby[g], Jonathan Tyler[a]

[a] Discipline of Earth Sciences, School of Physics, Chemistry and Earth Sciences, The University of Adelaide, Adelaide, SA, 5005, Australia
[b] Department of Oceanography, Noakhali Science and Technology University, Noakhali, 3814, Bangladesh
[c] Institute for Marine and Antarctic Studies (IMAS), University of Tasmania, Hobart, TAS, 7004, Australia
[d] School of Earth, Atmosphere and Life Sciences, The University of Wollongong, Wollongong, NSW, 2522, Australia
[e] Mawson Analytical Spectrometry Services (MASS), Faculty of Sciences, Engineering and Technology, The University of Adelaide, Adelaide, SA 5005, Australia
[f] Australian Nuclear Science and Technology Organisation (ANSTO), Lucas Heights, New South Wales, 2234, Australia
[g] Department of Geography, Environment and Population, School of Social Sciences, The University of Adelaide, Adelaide, SA, 5005, Australia

ARTICLE INFO

Handling Editor: Dr P Rioual

Keywords:
Ostracods
Megadrought
Stable isotopes
Common era
Charcoal
SAM

ABSTRACT

Understanding past hydroclimate variability through high-resolution records is key to assessing the recurrence of extreme climatic events, including prolonged droughts and floods and for sustainable environmental and economic planning. This study presents a sub-decadal-scale hydroclimate reconstruction based on oxygen isotope analysis of ostracod valves, extracted from the sediments of Lashmars Lagoon, Kangaroo Island, South Australia. Sediment dating was based on 19 accelerator mass spectrometry (AMS) radiocarbon (^{14}C) dates from pollen and plant macrofossils, alongside lead-210 and plutonium concentration analyses. Spanning the last ~2000 years, the oxygen isotopes record a series of multi-decadal wet and dry periods, manifest in the relative precipitation-evaporation balance of the lake. Of note, the record implies periods of prolonged declines in water balance, tentatively interpreted as droughts, from ~525 to 575 CE, ~770–790 CE, ~825–850 CE, and ~980–1020 CE. By contrast, the periods from ~150 to 450 CE and ~600–750 CE were relatively wet. Unfortunately, ostracods were absent within the sediments deposited between ~1250 and 1590 CE and as a result, no hydroclimatic pattern could be determined for this time period. The period from ~1590 to 1800 CE appears to have been notably dry, prior to an increase in effective moisture during the last 200 years. The Lashmars Lagoon record exhibits similar trends to a record from Blue Lake, Mt. Gambier, approx. 500 km to the southeast. However, these records contrast with other hydroclimate records from further east, implying a complex relationship with regional climate drivers. Comparison with instrumental period rainfall data, and reconstructed indices for major ocean–atmosphere interactions suggests that periods of increased moisture balance on Kangaroo Island were influenced by a combination of Southern Ocean and Indian Ocean derived climate drivers.

1. Introduction

Australia experiences a range of extreme climatic events including droughts, floods, and bushfires (Binskin et al., 2020). These natural events significantly impact the infrastructure, economy, ecosystems, agriculture, communities, and cultural heritage values of the country (Binskin et al., 2020). Among the aforementioned hazards, drought is a frequent and prevailing hydroclimatic feature in Australia (Kiem et al., 2016; Kiem and Austin, 2013). Since the late 19th century, Australia has experienced four major droughts, the "Tinderbox Drought" from 2017 to 19 CE, the "Millennium Drought" from 1997 to 2010 CE, the "World War II Drought" from 1935 to 1945 CE, and the "Federation Drought" from 1895 to 1905 CE (CSIRO and Bureau of Meteorology, 2015; Devanand et al., 2024; Murphy and Timbal, 2008; Verdon-Kidd and Kiem, 2009). The Millennium Drought is often referred to as the worst drought in the history of south-eastern Australia (Van Dijk et al., 2013), with

* Corresponding author. Discipline of Earth Sciences, School of Physics, Chemistry and Earth Sciences, The University of Adelaide, Adelaide, SA, 5005, Australia.
E-mail address: mahfuzur.rahman@adelaide.edu.au (M. Rahman).

https://doi.org/10.1016/j.quascirev.2025.109443
Received 12 February 2025; Received in revised form 21 May 2025; Accepted 21 May 2025
Available online 27 May 2025

widespread economic and ecological impacts (Leblanc et al., 2012). The Tinderbox Drought (2017–2019) was an extremely harsh event in Australia, severely affecting water availability, harming agriculture and ecosystems, and contributing to the devastating Black Summer bushfires in southeast Australia (Devanand et al., 2024). The combined economic losses from this drought and the following 2019–2020 CE bushfire crisis were estimated at A$63 billion (Wittwer and Waschik, 2021). In contrast, the past two decades have also seen significant flooding events across parts of Australia including Queensland in 2011, 2019 and 2022 CE (Palmer et al., 2023), as well as 2025. The occurrence of both severe floods and droughts in recent years has sparked discussions on their underlying causes and recurrence, emphasizing the importance of improving our understanding of multidecadal climate variability, especially over centennial to millennial timescales (Palmer et al., 2023).

Long-term past hydroclimate records, covering multi-decadal to centennial timescales, are crucial for calibrating climate models, assessing sensitivity to external forces, and evaluating the likelihood of prolonged extreme events (Barr et al., 2014; Chamberlayne et al., 2023; Cook et al., 2016; Kiem et al., 2016). Extending instrumental records with palaeoclimate datasets enhances our ability to develop robust and locally specific estimates of extreme event frequency, which are valuable for ecological management (Palmer et al., 2023; Saunders and Taffs, 2009). Despite these benefits, the spatial and temporal patterns of hydroclimate variability in southern Australia over the past two millennia remain uncertain. This uncertainty largely stems from the limited availability of long tree-ring chronologies and the geographically restricted distribution of lake and speleothem records (Dixon et al., 2017; Neukom and Gergis, 2012). As a result, alternative approaches to reconstructing Australian hydroclimate variability have incorporated distant records, including Antarctic ice cores and Chinese speleothems (Goodwin et al., 2014; McGowan et al., 2009; Tozer et al., 2016; Van Ommen and Morgan, 2010; Vance et al., 2013). Yet, significant uncertainties remain regarding the stability of climate teleconnections when extended beyond the calibration period and geographic scope (Dätwyler et al., 2018; Gallant et al., 2013).

Teleconnections between major ocean-atmospheric climate drivers influence extreme climatic events in Australia, in particular the Southern Annular Mode (SAM), the El Niño–Southern Oscillation (ENSO), the Indian Ocean Dipole (IOD) and the Interdecadal Pacific Oscillation (IPO) (Cai et al., 2011; Dey et al., 2021; Gouramanis et al., 2013; Hughes, 2003; Quigley et al., 2010; Risbey et al., 2009). The Southern Annular Mode (SAM), in both its positive and negative phases, is the dominant climate variability pattern in the Southern Hemisphere, controlling latitudinal rainfall distribution and temperature patterns from the subtropics to Antarctica (Abram et al., 2014). Several studies have linked positive phases of SAM with a southward shift of the Southern Westerly Winds (SWW) and decreased rainfall in southeastern Australia (Cai and Cowan, 2006; Hendon et al., 2007; Risbey et al., 2009). ENSO (El Niño & La Niña) related rainfall variability occurs predominantly in the north and east of Australia (Power et al., 2006). The IOD (positive & negative phases) particularly influences rainfall in southwest and southeast areas of Australia (Risbey et al., 2009). The Interdecadal Pacific Oscillation (IPO) plays a key role in modulating ENSO variability, particularly in Queensland (Cai et al., 2010; Kiem and Franks, 2004; Power et al., 1999).

Kangaroo Island (traditionally known as Karti or Karta), South Australia, is a region heavily impacted by drought and bushfires in recent decades, including devastating bushfires in 2019–20, which burnt more vegetation than any previously recorded fire on the island (Country Fire Service, South Australia). The sediments of Lashmars Lagoon, on the eastern margin of Kangaroo Island, offer an important archive of past environmental change on the island, since the seminal research by Clark (1983). Recently, Duxbury et al. (2024) described a continuous ~7000-year archive of environmental change from Lashmars Lagoon from a new series of sediment cores. Duxbury et al. (2024) argued that changes in the Leeuwin Current, which brings warm tropical waters to southern Australia, acted as an important influence on rainfall variability on Kangaroo Island through the last 7000 years, with a teleconnection to the El Niño Southern Oscillation. Importantly, Duxbury et al. (2024) demonstrated that the sediments of Lashmars Lagoon accumulated rapidly in recent millennia, with ~2.5 m of sediment spanning the last ~2000 years. In this study, we analysed oxygen isotope ratios of ostracod carbonate valves from Lashmars Lagoon, with a specific focus on the Common Era (last 2000 years), to constrain decadal-centennial scale hydroclimate variability in the region and evaluate the drivers of hydrological change in the context of regional climate variability.

2. Materials and methods

2.1. Study area

Lashmars Lagoon is located on the Dudley Peninsula in the far east of Kangaroo Island, bounded by latitude 35.801747°S – 35.812987°S and longitude 138.059007°E – 138.067108°E (Fig. 1). Kangaroo Island is the third largest island in Australia covering 4430 km^2 (Robinson and Armstrong, 1999). The island is visible from the South Australian mainland and is separated by the Investigator Strait and Backstairs Passage. Kangaroo Island is a culturally significant place for Traditional Owners, whose cultural knowledge and archaeological evidence suggest that permanent human occupation of the island ceased sometime after ~4300 cal a BP (Lampert, 1981; Walshe, 2005). Lashmars Lagoon is a nationally important wetland in South Australia (Environment Australia, 2001).

During fieldwork in September 2020, Lashmars Lagoon water was brackish (PSU: 7.40 and conductivity: 12,790 μS/cm) with a pH of 9.9. A bathymetric survey indicated largely uniform, flat bottomed lagoon with a maximum water depth of ~90 cm. The δ^{18}O and δ^{2}H of lake water was measured as +0.13 ‰ and −1.77 ‰ respectively. The lake has been known to dry out completely during some summers, most dramatically during early 2025, though the surface sediment at the centre of the lake remained wet (Clark, 1976). Lashmars Lagoon is located approximately 2 km inland from the shoreline, with the surrounding landmass about 7–26 m above mean sea level (MSL) according to Google Earth. The lake level is shown as 2 m above MSL, while the sea level is ~1 m below MSL (Google Earth). With a maximum water column depth of ~90 cm, this suggests that the lake floor is more than 2 m above MSL. As a very shallow lake located approximately 2 km inland from the shoreline and surrounded by landmass ranging from ~7 to 26 m above MSL, we assume that the lagoon floor is not connected to a salt wedge, unless the sea level was significantly higher in the past. Regional estimates of sea level change during the late Holocene, such as optically stimulated luminescence (OSL) ages of beach ridges at Seven Mile Beach, southeast Tasmania, suggest declining sea levels at ~0.4 m/yr from ~3600 to ~150 years ago (Oliver et al., 2017, 2022). Additionally, Dougherty (2018) suggested that this progradation may have been driven by sea-level fall from ~3500 to ~1000 cal a BP ago, based on sea-level curves from mainland Australia. There is currently no evidence that these sea level changes apply to coastal Kangaroo Island. However, if the magnitude of these sea level changes are comparable, this would suggest that during the Holocene the lake floor at Lashmars Lagoon was lower than sea level, and that there may have been a marine influence at a point in the past, although the sedimentary evidence to date does not imply this (Duxbury et al., 2024).

Lashmars Lagoon is part of a relatively small catchment area of about 60 km^2, most of which has undergone gradual land clearing since the early 1820s on the Dudley Peninsula and its vicinity (Taylor, 2008). As of 2013, farmland accounted for 60 % of the catchment, although native vegetation still fringes the lagoon (Environmental Protection Agency, 2013). Three primary creeks supply water to the lagoon, differing in their flow permanence. The most consistent is a small, unnamed creek in the northwest, followed by the larger Chapman River to the southwest,

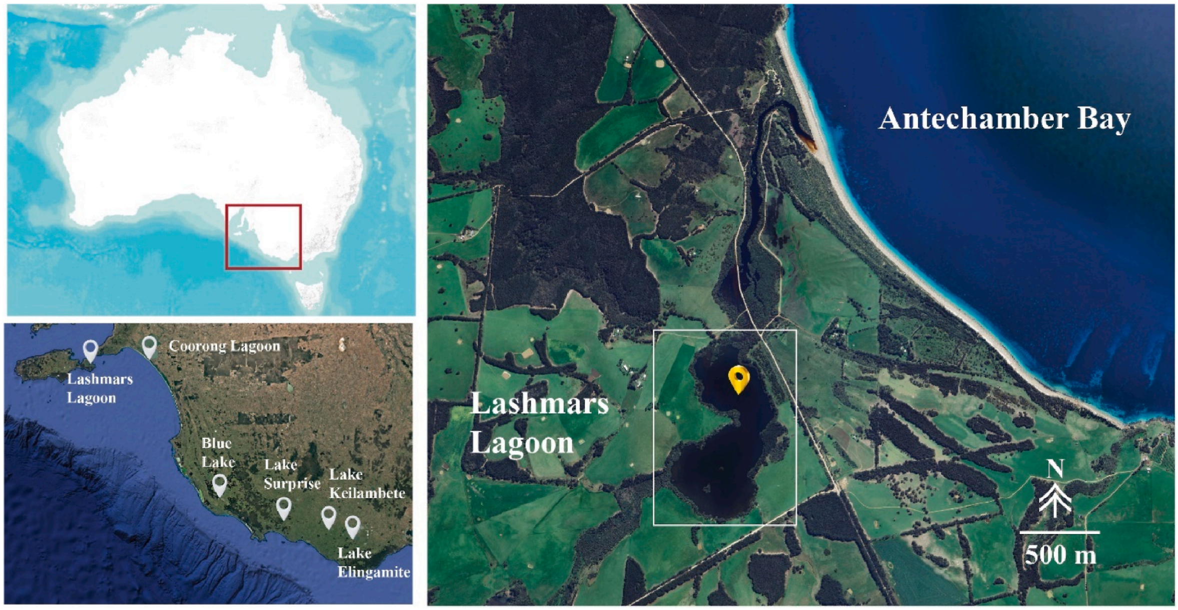

Fig. 1. Location map of the study area. Coring was conducted within a ~5 m radius of the yellow icon on the lagoon. Service layer credits: Esri, Maxar, GeoEye, Earthstar, Geographics, CNES/Airbus DS, USDA, USGS, AeroGRID, IGN, and the GIS user community. (For interpretation of the references to colour in this figure legend, the reader is referred to the Web version of this article.)

while the southeastern creek remains ephemeral and flows primarily in winter (B. Cooter, personal communication, 2021). The lagoon discharges downstream through Chapman River to the northeast, continuing for approximately 3 km before reaching a beach berm that is rarely breached, even after heavy rainfall or storm events (Clark, 1976).

The surface geology of the Lashmars Lagoon catchment is mainly composed of the Holocene alluvial floodplain and fan deposits belonging to the Coonambidgal Formation (Source: SARIG). The nearest weather station is Cape Willoughby lighthouse where, for 30 years (1993–2022), annual mean rainfall was 493 mm/year and the annual average minimum and maximum temperature recorded was 13.1 °C and 18.4 °C (Bureau of Meteorology, 2023).

2.2. Core recovery and preparation

Sediment cores were collected in September 2020 using a Bolivia piston corer fitted with a 1 m long PVC pressure pipe (Wright, 1967). Three overlapping cores were collected in ~1 m increments at three locations (LAS20-2, LAS20-3, and LAS20-4), located within a ~5 m radius. An additional gravity core (LAS20-1; Pylonex HTH; Renberg and Hansson, 2008) was used to retrieve the sediment-water interface, subsampled in the field at 2.5 mm intervals. Among them, cores LAS20-1, LAS20-3, and LAS20-4 was used in this study (Fig. 2). A detailed description of core recovery and sample processing is given in Duxbury et al. (2024). The Bolivia core sections were longitudinally split and visually examined for their colour, grain size, structure, consistency, and macrofossil content. Core correlation was carried out based on bromine (Br) Itrax µXRF data, because of its strong association with organic matter and its distinctive stratigraphic pattern (Pashkova et al., 2016; Seki et al., 2019) (Fig. 2). Following the methodology detailed by Francke et al. (2017), the correlation process utilised the software packages CORRELATOR (cse.umn.edu/csd/correlator) and CORELYZER (cse.umn.edu/csd/corelyzer) to develop a composite depth scale (Fig. 2).

2.3. Chronology

The development of the full 7000-year sediment age-depth model is described in detail by Duxbury et al. (2024). Previous radiocarbon

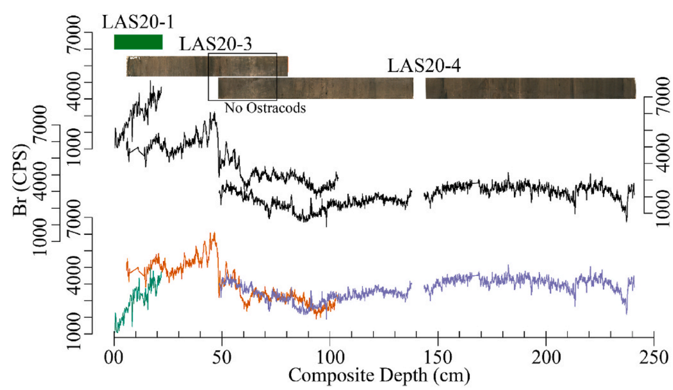

Fig. 2. Itrax-derived optical images of cores LAS20-3 and LAS20-4 (LAS20-1 not imaged) and Br concentration in counts per second (CPS) for each of the cores analysed in this paper, as described in detail by Duxbury et al. (2024). In lower panel, green data = LAS20-1 (analysed as discrete samples); orange data = LAS20-3 and purple data = LAS20-4. Overlapping sediment from both LAS20-3 and LAS20-4 were inspected to confirm the absence of ostracod valves in the section indicated by a black box. (For interpretation of the references to colour in this figure legend, the reader is referred to the Web version of this article.)

analyses were conducted on cores LAS20-3 and LAS20-4, while Pb and Pu analyses were conducted on core LAS20-2. As the current research was aimed at establishing a high-resolution hydroclimate record for the last ~2000 years, 12 additional radiocarbon dates for the upper 2.5 m of sediment (cores LAS20-3, LAS20-4) were analysed from pollen concentrates, following Cadd et al. (2022), which were subsequently converted to graphite targets for AMS analysis (Hua et al., 2001; Wilcken et al., 2015). A revised sediment age-depth model was developed using the rPlum package in R, integrating both new and previously published (Duxbury et al., 2024) dates for the composite core profile. This package applies Bayesian statistics to combine ^{210}Pb and radiocarbon dates (Aquino-López et al., 2018; Blaauw and Christen, 2011). As per Duxbury et al. (2024), this model was anchored using the coring date of September 2020 and the year 1964 CE, based on the depth of maximum increase in Pu concentration, reflecting fallout from nuclear weapons testing (Walling and Meyers, 2012). Radiocarbon dates were calibrated against the SHCal20 calibration curve (Hogg et al., 2020) and are reported in calibrated years before present (cal a BP), where 'present' is 1950 CE. The ages reported in this manuscript are the weighted mean of potential ages for each depth, with associated uncertainties as inferred from the Monte Carlo simulation.

2.4. Ostracod extraction

Samples were processed for ostracod extraction from contiguous 0.25 cm intervals for core LAS20-1 and 1 cm intervals for LAS20-3 and LAS20-4. For each level, a ~1 cm^3 sample of wet sediment was freeze-dried for 24 h and then 5 % sodium hexametaphosphate $Na_6[(PO_3)_6]$ was added and left overnight at ~20 °C to deflocculate the clay particles. Samples were sieved through a 125 μm steel mesh using deionised water and >125 μm fractions were again freeze-dried for 48 h. A stereo microscope was used to view the ostracod valves which were then picked using a fine nylon brush. Ostracod valves were cleaned using a fine nylon paintbrush and methanol to remove adhering sediment. Representative high-resolution pictures were prepared through stacking multiple images at different focus levels together and captured in the Invertebrate Systematics and Biodiversity Lab, School of Biological Sciences at The University of Adelaide. Ostracod taxonomy was determined following De Deckker (1981, 1983) and confirmed through personal correspondence with Prof. Patrick DeDeckker.

2.5. Stable isotope analyses

Pre-cleaned valves of single adult ostracod species (where available), between 60 and 140 μg valves per sample, were weighed into glass vials using a Sartorius Micro Balance CUBIS® II. In many cases, there was no intact valve to isolate and for those samples, multiple adult ostracod broken valves (ranging from two to six, with the majority being three to four) of *Mytilocypris mytilodes* and *Mytilocypris praenuncia* were used for isotope analyses. No adult and juvenile valves were combined for isotope analyses. A total of 377 oxygen and carbon isotope analyses were conducted on 235 ostracod samples. Among them, 132 replicate analyses were performed on 90 randomly selected samples, with the number of replicates per sample ranging from 1 to 12. A total of 54 replicates from 8 samples were conducted to examine any isotope offsets between ostracod species. In most cases, *M. mytiloides* and *M. praenuncia* were analysed. *Alboa worooa* was analysed in 22 samples, while *Candonocypris novaezelandiae* was analysed in only two instances. *Diacypris spinosa* was not used due to the unavailability of larger valves. Stable isotope ratios ($^{18}O/^{16}O$ and $^{13}C/^{12}C$) were measured using a Nu Perspective isotope ratio mass spectrometer coupled to a Nu Carb acid preparation system, located in the Mawson Analytical Spectrometry Services (MASS) at The University of Adelaide. Oxygen and carbon isotope data are reported as $\delta^{18}O_{ostracod}$ and $\delta^{13}C_{ostracod}$ relative to the Vienna Pee Dee Belemnite (VPDB) standard using the standard delta (δ) notation in parts per mille (‰). Analytical precision was calculated by repeated measurement of internal standards ANU P3 and UAC-1 and reference materials CO-1 and CO-8, and average standard deviation values were found 0.024 ‰ and 0.042 ‰ for $\delta^{13}C$ and $\delta^{18}O$ respectively.

3. Results

3.1. Sediment lithology and chronology

The sediment cores from Lashmars Lagoon are primarily composed of fine-grained, organic-rich, clay-dominated deposits, exhibiting a homogenous texture. Their colouration varies from greys and black to brown and olive. No visible signs of hiatuses or erosional surfaces were observed (Duxbury et al., 2024).

A Bayesian age-depth model for the full composite 728 cm sediment profile was constructed using new (Table 1) and previously published radiocarbon dates from Duxbury et al. (2024) using the rplum package in R (Aquino-López et al., 2018; Blaauw and Christen, 2011) (Supplementary Fig. 1). As the current study is focused on the last 2000 years, the revised age model for the upper 262 cm of sediment is presented and described here (Fig. 3). This age-depth model incorporates 19 radiocarbon and 12 ^{210}Pb dates. Radiocarbon analyses on samples from cores LAS20-3 and LAS20-4 (28 cm–261.9 cm in the composite depth profile) generally display a pattern of increasing age with increasing depth within the uncertainty of calibrated ranges. ^{210}Pb dates, reported in Duxbury et al. (2024), returned unsupported ^{210}Pb concentrations that decreased with depth. The results of AMS radiocarbon dating and ^{210}Pb analyses are summarised in Table S1 in the Supplementary Information. The model is anchored with the coring date (September 2020) at 0 cm and the Pu-isotope inferred bomb peak at 1964 CE at 13.5 cm (Duxbury et al., 2024). The Bayesian rplum model, combining all three dating methods, returned a modelled age of the deepest sample analysed in this study (composite depth 243.2 cm) with a median age of 1969 cal a BP (19 BCE; range 1875–2088 cal a BP). The calculated sediment accumulation rate ranged from 0.9 to 1.4 mm/year.

3.2. Ostracods in the Lashmars Lagoon sediments

A total of five ostracod species were identified in the sediments of Lashmars Lagoon. The species are *Mytilocypris mytiloides* (Brady, 1886), *Mytilocypris praenuncia* (Chapman, 1936), *Diacypris spinosa* (De Deckker, 1981), *Alboa worooa* (De Deckker, 1981), and *Candonocypris novaezelandiae* (Baird, 1843) (Fig. 4A).

Ostracods exhibited a patchy distribution throughout the sediment

Table 1
New radiocarbon dates for samples from the Lashmars Lagoon cores (LAS20-3, LAS20-4).

ANSTO	Sample Type	Composite Depth (cm)	$\delta^{13}C$ per mil	percent Modern Carbon	Conventional ^{14}C Age	Calibrated ^{14}C Age
			$\delta^{13}C$ 1σ	pMC 1σ	a BP 1σ	Min – Max (cal a BP)
OZBR36	Pollen	24	−25.0[a]	95.6 ± 0.77 C	360 ± 65	28–176
OZBR37	Pollen	42	−25.0[a]	94.15 ± 0.92 C	480 ± 80	247–385
OZBR39	Pollen	69	−25.0[a]	91.67 ± 0.65 C	700 ± 60	540–680
OZBR40	Pollen	83	−25.0[a]	88.49 ± 0.59 C	980 ± 55	687–838
OZBR42	Pollen	101	−25.0[a]	86.73 ± 0.55 C	1140 ± 60	841–965
OZBR43	Pollen	119.4	−25.0[a]	84 ± 0.69 C	1400 ± 70	992–1190
OZBR44	Pollen	133.4	−25.0[a]	81.57 ± 0.62 C	1640 ± 70	1110–1295
OZBR45	Pollen	139.4	−25.0[a]	83.87 ± 0.54 C	1410 ± 60	1177–1320
OZBR48	Pollen	182.2	−25.0[a]	80.92 ± 0.47 C	1700 ± 50	1440–1605
OZBR49	Pollen	196.2	−25.0[a]	78.6 ± 0.62 C	1930 ± 70	1542–1733
OZBR51	Pollen	224.2	−25.0[a]	77.62 ± 0.65 C	2030 ± 70	1735–1930
OZBR52	Pollen	237.2	−25.0[a]	77.71 ± 0.81 C	2030 ± 90	1826–2030

C- small mass corrected.
[a] assumed due to small mass.

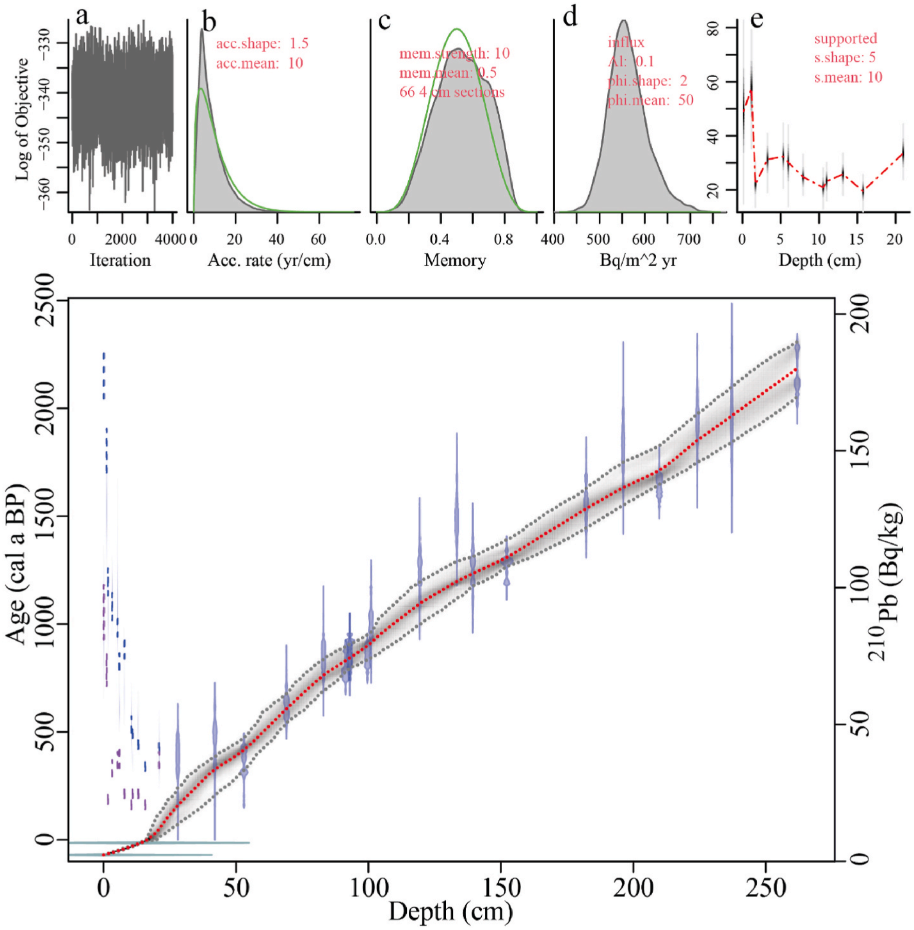

Fig. 3. Bayesian age-depth model, constructed using the package rplum in R. Blue markers depict probability distributions for radiocarbon-dated samples against the left axis. The small rectangles indicate the total (blue) and supported (purple) ^{210}Pb activity against the right axis, respectively. Green markers represent calendar ages assigned to the coring date and peak Pu concentration, following Duxbury et al. (2024). Grey dotted lines represent 95 % confidence intervals, with darker shading indicating the most likely ages. The red dotted line shows the weighted mean age. Upper panels indicate: a. the model stability (log of objective) as a function of model iteration performed; the model priors (green) and posteriors (grey) for b. the modelled sediment accumulation rate; c. the memory function used to construct the model; d. the influx of ^{210}Pb; and e. the posterior supported activities of ^{210}Pb at every depth. Red text indicates the model settings. (For interpretation of the references to colour in this figure legend, the reader is referred to the Web version of this article.)

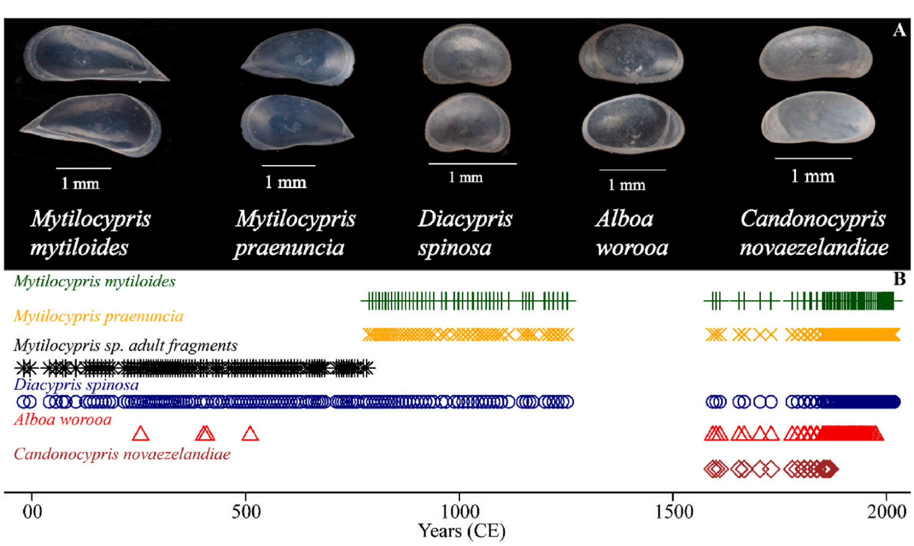

Fig. 4. Ostracod species identified from the Lashmars Lagoon sediments (A) and their presence or absence throughout the composite profile (B). Images represent stacked optical images through different focal distances.

profile (Fig. 4B). The youngest ostracod fossils were found at a composite depth of 0.875 cm with a corresponding age of 2017 CE. Adult and intact ostracods were found in moderate to abundant concentrations in each sample between 0.875 and 45.4 cm composite depth (~2017–1590 CE). *Mytilocypris mytiloides*, *M. preanuncia*, and *D. spinosa* were common in this section. *Alboa worooa* was found within the depth range of 12–45.4 cm (~1590–1974 CE) but was particularly abundant between 22.375 and 45.4 cm (~1590–1875 CE). *Candonocypris novaezelandiae* (2–5 valves per sample) were found within the depth range 23.125–45.4 cm (~1590–1861 CE). Between 45.4 and 76.4 cm (~1250–1590 CE), the samples did not contain any ostracod valves, either broken or intact.

Between 77.4 and 128.4 cm (~787–1250 CE), the quantity of intact valves of *M. mytiloides* and *M. praenuncia* decreased, and the proportion of broken valves increased. The small-sized ostracod *D. spinosa* was present in almost all of these samples. Between 129.4 and 243.2 cm (~19 BCE – 780 CE), the quantity of both intact and broken valves in the sediment was very low. As a result, ostracod identification to species was not possible for the majority of these samples except *D. spinosa*. However, it was possible to discern that the genus of broken valves was *Mytilocypris,* either *M. mytiloides* or *M. praenuncia*. Intact *A. worooa* was found at occasional depths: 170.2 cm, 184.2 cm, 185.2 cm, and 209.2 cm (~511 CE, ~408 CE, ~401 CE, and ~254 CE respectively).

Overall, the distribution of the ostracods in sediment cores can be divided into four composite depth intervals: a) Higher concentration of intact ostracod valves between the surface and 45.4 cm; b) No ostracod valves between 46.4 and 76.4 cm; c) Fewer intact valves but comparatively more abundant broken valves between 77.4 and 128.4 cm; and d) Very low intact as well as broken valves between 129.4 and 243.2 cm (Fig. 4B). In addition to the large gap in ostracod preservation between 46.4 and 76.4 cm, there were a few small depth intervals of 1–3 cm where ostracods were not found. Except for the depths between 45.4 and 76.4 cm, where no ostracods were found, almost all samples contained juvenile *D. spinosa* and, in some cases, four other species. This suggests that the ostracods were not transported by strong inflows from a river upstream.

3.3. Oxygen and carbon isotope composition of fossil ostracods

A total of 377 oxygen and carbon isotope analyses were made from 235 ostracod samples. Oxygen isotope ($\delta^{18}O_{ostracod}$) values ranged from −1.7 to 9.5 ‰ with a mean value of 4.3 ± 1.7 ‰ and carbon isotope ($\delta^{13}C_{ostracod}$) values ranged from −13.4 to −1.5 ‰ with a mean value of −7.9 ± 2.1 ‰. Among them, 132 replicates were made from 90 randomly selected samples and the number of replicates ranged from 1 to 12 per sample. These replicates were made to determine whether data from different species picked from the same sample are statistically similar or not.Though $\delta^{18}O_{ostracod}$ from different species within the same sample exhibited variable values, the T-test results revealed that the $\delta^{18}O_{ostracod}$ values are statistically similar (not significant) ($p = 0.44$) between M. *mytiloides* and M. *praenuncia*. *Mylitocypris mytiloides* and *A. worooa* also presented a statistically similar (not significant) result ($p = 0.26$) (T-test results between data sets are given in Supplementary Information, Table S2). *Mytilocypris mytiloides* and *M. praenuncia* are closely related species and in many cases it was not possible to discern whether it was either *M. mytiloides* or *M. praenuncia*. Additionnaly, a T-test revealed their $\delta^{18}O$ values are statistically similar. Therefore, their $\delta^{18}O$ values has been presented combinedly (Fig. 5a). Although *M. mytiloides* and *A. worooa* $\delta^{18}O$ exhibited statistically similar values, they are different genera. As a result, their $\delta^{18}O$ values are shown separately to assess their influence on the combined *M. mytiloides* and *M. praenuncia* record (Triangle symbol in Fig. 5a). *Candonocypris novaezelandiae* was analysed in only two instances from the same sample and is presented in Fig. 5a using diamond symbol. The $\delta^{18}O$ data from *A. worooa* covers only a short time period (~1940–1800 CE) compared to the last 2000 years. It has minimal impact on the combined

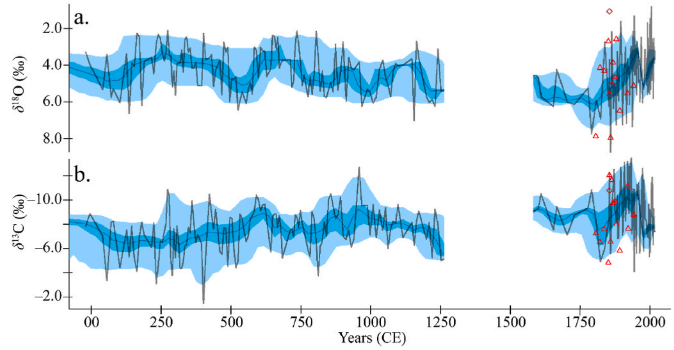

Fig. 5. $\delta^{18}O_{ostracod}$ and $\delta^{13}C_{ostracod}$ values plotted for the combined *M. mytiloides* and *M. praenuncia* species over the last ~2000 years. Values for *A. worooa* and *C. novaezelandiae* are also shown by triangle and diamond symbols, respectively. The light blue shading represents the 95 % confidence interval for age uncertainty, while the dark blue shading corresponds to the 68 % confidence interval. Fine grey lines depict the weighted mean of 2000 time series ensembles, whereas thick grey lines show the original published data in relation to the weighted mean age model. (For interpretation of the references to colour in this figure legend, the reader is referred to the Web version of this article.)

M. mytiloides and *M. praenuncia* record and does not change the overall interpretation of regional hydroclimatic change (Supplementary Fig. 2). These observations support the use of combined $\delta^{18}O$ data from all species as a hydroclimatic proxy in this instance. The temporal resolution of $\delta^{18}O_{ostracod}$ data varies slightly down-core due to the absence of ostracod valves in some sediment samples. For the sediments dated between ~1810–2017 CE, a total of 90 samples were analysed with sample resolution ranged from 0.48 to 12.4 years. From ~1800 to 1590 CE only nine samples could be analysesd due to missing ostracods in sediments and temporal resolution ranged from 7.59 to 53.16 years. Between ~19 BCE – 1250 CE a total of 136 samples were analysed with a temporal resolution range from 5.47 to 44.33 years. Overall, excluding the gap with no ostracods (~1590–1250 CE), the average sample resolution is 7.12 years. By calculating the mean $\delta^{18}O_{ostracod}$ for each sample, several periods of higher and lower $\delta^{18}O_{ostracod}$ can be observed for the last ~2000 years (Fig. 5a). Higher $\delta^{18}O_{ostracod}$ values were observed between ~19 BCE – 140 CE, ~460–600 CE, ~750–870 CE, ~960–1060 CE and ~1590–1800 CE. Periods of lower $\delta^{18}O_{ostracod}$ were observed between ~140 and 460 CE, ~600–750 CE, ~870–950 CE, and ~1060–1250 CE. In general, the mean $\delta^{18}O_{ostracod}$ values varied by ± 1 ‰ about an average of ~4 ‰, with a gradual trend of increasing $\delta^{18}O_{ostracod}$ between ~0 and 1250 CE, a period of high $\delta^{18}O_{ostracod}$ between ~1600 and 1800 CE and a trend towards lower $\delta^{18}O_{ostracod}$ between ~1800-present (Fig. 5a). From the beginning of the common era to ~1250 CE, it is clear that periods of lower $\delta^{18}O_{ostracod}$ were comparatively longer (approximately 750 years) than periods of higher $\delta^{18}O_{ostracod}$ (~500 years).

Carbon isotope ($\delta^{13}C_{ostracod}$) values are presented in a similar manner to $\delta^{18}O$ (Fig. 5b); however, $\delta^{13}C$ does not covary with $\delta^{18}O$, with a correlation coefficient of 0.038. In open lake systems, $\delta^{13}C$ values typically exhibit more erratic behavior (Talbot, 1990), which may be influenced by dissolved inorganic carbon in the lake water, microhabitat effects, and species-specific vital offsets (Von Grafenstein et al., 1999). Consequently, interpreting $\delta^{13}C$ is more complicated (Decrouy et al., 2011; Pérez et al., 2013). Given that Lashmars Lagoon is an open lake system and $\delta^{13}C$ shows no correlation with $\delta^{18}O$, $\delta^{13}C$ values were not used for palaeohydrological interpretation in the present study.

4. Discussion

4.1. Modern ecology of ostracod taxa in Lashmars Lagoon sediments

All five ostracod species identified in the Lashmars Lagoon sediments are non-marine, of the family Cyprididae. Overall, their presence indicates that through the last 2000 years, Lashmars Lagoon was a brackish to fresh wetland, likely subjected to seasonal salinity fluctuations analogous to those observed today. This inference is consistent with the relatively high surface area to volume ratio of the shallow lagoon, which promotes summer evaporative enrichment and winter flushing by freshwater stream discharge. The lagoon does not currently receive marine influx, and the known ecology of the ostracod taxa suggests that a marine influence was not prevalent throughout the studied period. For example, the dominant taxa in the record – *M. mytiloides* and *M. praenuncia* are found in a wide range of permanent and temporary fresh, brackish and saline environments, but not in marine ecosystems (De Deckker, 1983, 1981, p-151; Rahman et al., 2023). *Mytilocypris mytiloides* has a salinity tolerance ranging from 1.3 to 172.9 g/L, with a median salinity optimum of ~19 g/L, while *M. praenuncia* tolerates salinities from 4 to 51.1 g/L, with the highest median optimum also around ~19 g/L (Rahman et al., 2023). *Diacypris spinosa* is generally found in ephemeral or permanent salt lakes across Australia but is absent in lakes where salinity remains consistently above 20 ‰ (De Deckker, 1981, p-98). *Alboa worooa* inhabits lakes and temporary pools that may sometimes hold mildly saline water, reaching up to 5 ‰ (De Deckker, 1983, 1981, p-45). *Candonocypris novaezelandiae* is a freshwater species typically found in permanent and semi-permanent pools and dams. While adults are strictly benthic and have never been observed swimming, juveniles are strong swimmers (De Deckker, 1981, p-80).

4.2. Possible reasons for missing ostracods

Our ability to derive a high-resolution, continuous record of hydroclimate variability relies on the continued accumulation of ostracods within the sediments. Unfortunately, no ostracods were found in the sediment samples of Lashmars Lagoon dated to between ~1250 and 1590 CE, as also indicated by the low concentration of Ca (as $CaCO_3$) in the sediment (Fig. 6b). As well as ostracods, carbonate gyrogonites are also abundant in the Lashmars Lagoon sediments, yet these too are

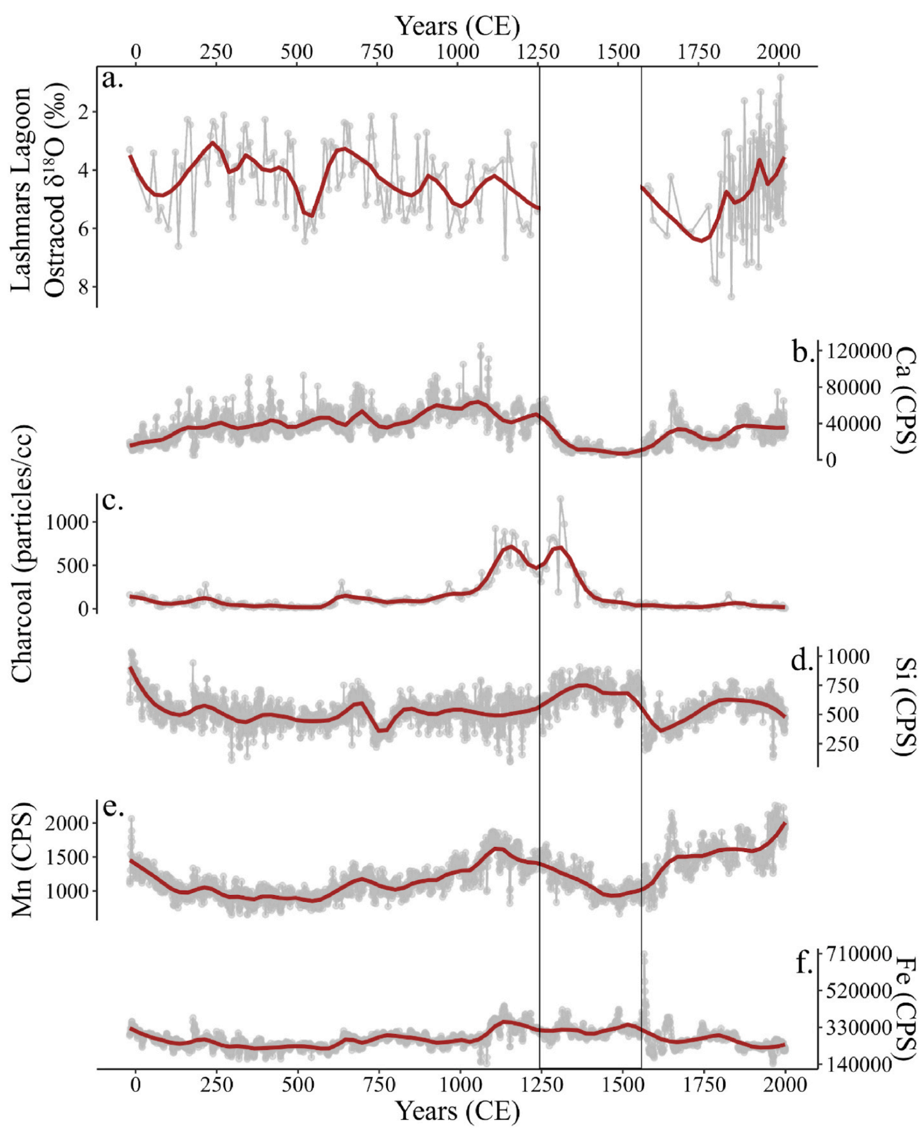

Fig. 6. Ostracod oxygen isotope data, illustrating the gap in ostracod preservation between ~1250 and 1590 CE (a) compared to the concentration of Ca (b), Si (d), Mn (e), and Fe (f) measured using ITRAX µXRF core scanning in counts per second (CPS), reported by Duxbury et al. (2024). Also shown is charcoal concentration in particles per cm^3 (c) from Duxbury (2022). Red lines indicate a locally weighted sum of squares (loess) fit with span = 0.1 (Cleveland et al., 2017). This span of 0.1 is used for all cases in this manuscript. (For interpretation of the references to colour in this figure legend, the reader is referred to the Web version of this article.)

absent in this particular unit. Gyrogonites are the calcified outer crust of oospores, which are non-calcified spores produced by charophytes – in this case possibly of the genus *Lamprothamnium* (A. García, pers. comm) (García, 1987; Leitch, 1989; Soulié-Märsche and García, 2015). Oospores and gyrogonites are frequently found in articulated pairs in the Lashmars Lagoon sediments (Fig. 7a–c), however in the sediments dated ~1250–1590 CE, while gyrogonites are absent, oospores remain abundant, indicating that charophytes were still present in the lagoon at this time. This pattern implies that either the calcified gyrogonites were dissolved due to lower pH, either in the lake water or sediment pore water, or that gyrogonites could not form due to low pH and carbonate ion concentration. Encrustation of charophytes as well as gyrogonites is predominantly dependent on calcium concentrations and pH in lake water (Herbst et al., 2018). Charophytes normally grow in lake water with a minimum calcium concentration of 8.2 mg/L (Kufel et al., 2016) and pH > 8 (Anadón et al., 2002). On the contrary, the dissolution of carbonate encrustation is facilitated by decreasing the pH and saturation index of calcite in lake water (Strzałek et al., 2024). At the time of coring, Lashmars Lagoon water was brackish (PSU: 7.40 and conductivity: 12,790 μS/cm) with a pH of 9.9, which is very suitable for gyrogonite growth but for some reason these conditions were absent in Lashmars Lagoon between ~1250 and 1590 CE.

In organic-rich sediments, microbial degradation of organic matter can lead to oxygen (O_2) depletion and accumulation of metabolic carbon dioxide (CO_2) which leads to progressive acidification (Arvidson and Morse, 2014; Nesbitt and Mucci, 2021) and the dissolution of carbonate minerals (Kurganskaya and Churakov, 2018). A similar situation can arise following the century-long deposition of bushfire-produced charcoal, which can lower pH in both lake waters and sediments due to increases in SO_4^{2-}, albeit countered by a potential increase in base cations (Granath et al., 2021). Duxbury (2022) demonstrated a marked increase in charcoal concentration in the sediments of Lashmars Lagoon in the sediments dated ~1100–1350 CE (Fig. 6c). The beginning of this charcoal peak occurs prior to the absence of ostracods in the Lashmars Lagoon sediments, but it may signify a perturbation to the lake and catchment that influenced the chemistry of the lake water and sediment for the subsequent ~300 years. As an alternative, or possibly complementary mechanism, higher Si concentrations in the sediments dated ~1250–1550 CE indicate higher sand concentrations, which also suggest an increase in catchment erosion, possibly in response to the loss of vegetation. The increase in sand may have been responsible for the dilution of carbonate in the sediment and possible physical breakage of carbonate minerals (Fig. 6d). Similarly, the catchment erosion may have increased water turbididty. These factors do not explain the continued presence of charophyte oospores in the sediments, however, which imply that the charophytes persisted in the lake despite the absence of gyrogonites. A decreasing trend in Mn concentration (Fig. 6e) and a relatively higher concentration of Fe (Fig. 6f) can be observed during the period when ostracods are absent. Mn and Fe are well-known pH and redox-sensitive elements (Koinig et al., 2003). Studies on lake sediments by Carignan and Nriagu (1985) and Young and Harvey (1992) have demonstrated that low Mn concentrations in sediments are associated with lower water pH, which reduces particulate Mn by facilitating the diffusion of reduced Mn precipitates as insoluble oxides. Additionally, these studies suggested that higher Fe concentrations in acidic lake sediments result from the precipitation of Fe-humic substances from the water column. In short, the cause of absent ostracod and gyrogonite fossils between ~1250 and 1590 CE is uncertain but possibly relates to fire disturbance and associated change in lake water or sediment pore-water pH within the lake.

4.3. Interpretation and validation of ostracod $\delta^{18}O$ as a hydroclimate proxy at Lashmars Lagoon

Changes in the $\delta^{18}O_{ostracod}$ values reflect a combination of the $\delta^{18}O$ of lake water, water temperature, and species-specific 'vital' effects on carbonate-water oxygen isotope fractionation (Decrouy et al., 2011; Devriendt et al., 2017; Li et al., 2012; Li and Liu, 2010; Liu et al., 2009). Additional complexities include variation in the season of ostracod growth, inter-annual variability within a composite sample (in our case ~5–10 years), and the potential for growth in micro-habitats, such as freshwater springs within otherwise saline/evaporated lakes (Decrouy et al., 2011; Devriendt et al., 2017; Von Grafenstein et al., 1999).

Specific fractionation factors for the species analysed in this study, predominantly *M. mytiloides* and *M. praenuncia* have not been established to date. In this study, we demonstrated that while $\delta^{18}O_{ostracod}$ values do vary between taxa within individual samples, those $\delta^{18}O_{ostracod}$ values are not significantly different, and there is no consistent trend whereby one taxon exhibits higher or lower $\delta^{18}O$ than another (Table S2). Decrouy et al. (2011) reported that fractionation factors among different species within the family Cyprididae are similar. This supports the findings of the present study, as *Mytilocypris* belong to the Cypridae family. In general, the differences between $\delta^{18}O_{ostracod}$ for different taxa are equivalent to differences between $\delta^{18}O_{ostracod}$ of sequential samples of the same taxon. Therefore it is difficult to discern whether differences are due to different species-specific fractionation factors, or whether they relate to inherent spatial and temporal variability in the lake environment.

The effect of temperature on $\delta^{18}O$ within ostracod shell carbonate is relatively small ~0.21 ‰ per °C (Beck et al., 2005; Decrouy et al., 2011; Devriendt et al., 2017), close to inorganic calcite-water or bicarbonate-water oxygen isotope fractionation (Beck et al., 2005; Decrouy et al., 2011; Devriendt et al., 2017; Kim and O'Neil, 1997). As a result, the range of measured $\delta^{18}O_{ostracod}$ values (−1.7 to 9.5 ‰), is too high to be feasibly explained by temperature variability alone. By contrast, changes in lake water $\delta^{18}O$ on the order of >5 ‰ are commonplace on both seasonal and inter-annual timescales in Australian wetlands due to changes in the rainfall to evaporation hydrological

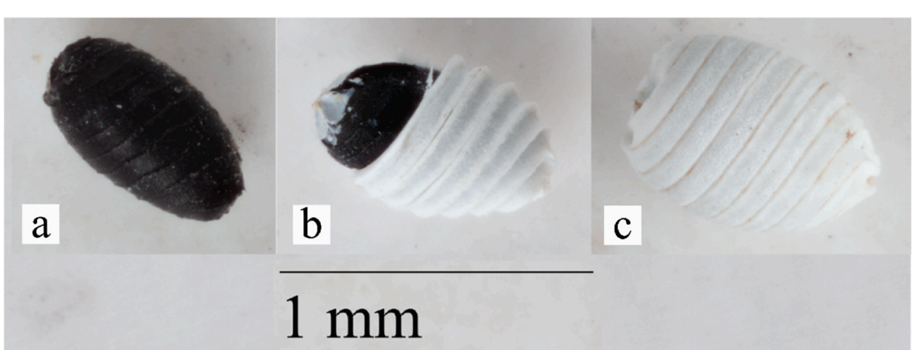

Fig. 7. Representative pictures of oospore (a), oospore partially covered by gyrogonite (b), and gyrogonite (c) extracted from the same sediment samples as ostracods.

balance (Ankor, 2020; Tyler et al., 2022). Increased rainfall amount can also lead to lower δ^{18}O values in rainfall (Dansgaard, 1964), as has been demonstrated across southern Australia (Fischer and Treble, 2008; Treble et al., 2005; Dixon, 2019). Furthermore, increased relative humidity can lead to decreased kinetic fractionation of lake water (Holmes et al., 2023). As a consequence, the combined effects of rainfall amount, and particularly the balance of inflow to evaporation, are the most likely drivers of $\delta^{18}O_{ostracod}$ variability at Lashmars Lagoon. We, therefore, focus our interpretation on the mean δ^{18}O of all ostracods analysed in each sample, as well as the multi-decadal scale variability in the $\delta^{18}O_{ostracod}$ signal, as an archive of multi-decadal hydroclimate variability. Similar interpretation of ostracod (Gouramanis et al., 2010, 2012; Wilkins et al., 2013) and mollusc δ^{18}O (Chamberlayne et al., 2023) has been made from wetland sediments in south-western Western Australia, coastal lagoon sediments from South Australia and lakes in South Australia and Victoria.

To validate the relationship between $\delta^{18}O_{ostracod}$ and regional climate variability, we compared our data from Lashmars Lagoon with instrumental climate records from the Australian Bureau of Meteorology (BoM), since 1880 CE (Fig. 8). Validating $\delta^{18}O_{ostracod}$ variability against instrumental climate records is challenging, due to imprecision in the sediment chronology, the integration of multiple years in the sediment record, likely seasonal or inter-annual bias within the sediment record and the potential impact of post-colonial anthropogenic impacts on lake and catchment hydrology. Nevertheless, a comparison of the sediment record with instrumental climate data over the period 1900–2020 CE can help clarify the interpretation of the sedimentary record deeper into the past.

Firstly, we explored the potential effects of changes in temperature and the δ^{18}O of precipitation on the δ^{18}O of ostracod valves. Temperature effects were estimated based on the carbonate-water fractionation factor described in Beck et al. (2005), Decrouy et al. (2011), and Devriendt et al. (2017), namely ~0.21 ‰ per °C. This equation was applied using the annual average air temperature from Cape Willoughby weather station, with the estimated mean-variance added to the mean $\delta^{18}O_{ostracod}$ deposited within the post-1900 sediments. These results are largely invariable throughout the last 120 years, suggesting that temperature would have imparted a negligible effect upon $\delta^{18}O_{ostracod}$ (Supplementary Fig. 3).

The effects of changes in the δ^{18}O of precipitation were considered using δ^{18}O values measured from a recent stalagmite collected from Kelly Hill Cave in western Kangaroo Island, which spans ~1911–2014 CE (Dixon, 2019). Speleothem δ^{18}O is commonly interpreted as reflecting the δ^{18}O of precipitation (Parker et al., 2021), albeit with some exceptions (Treble et al., 2005). The Kelly Hill Cave values exhibit a range of ±1 ‰ (Dixon, 2019), suggesting that changes in the δ^{18}O of precipitation also contributed a relatively small amount to the full range of $\delta^{18}O_{ostracod}$ variability, although it is possible that multi-annual accumulation of rainwater within the aquifer may have dampened the range of variability recorded in the speleothem. These observations lead to the conclusion that variability in the hydrological balance of evaporation vs. precipitation is the most likely cause of $\delta^{18}O_{ostracod}$ variability at Lashmars Lagoon. Given the aforementioned effects of changing P–E on lake water oxygen isotopes, we hypothesised that P–E is the primary driver of $\delta^{18}O_{ostracod}$ and would exhibit a negative correlation with $\delta^{18}O_{ostracod}$.

This hypothesis that $\delta^{18}O_{ostracod}$ relates to P−E is partly supported by the comparison between $\delta^{18}O_{ostracod}$ and P−E (Fig. 8). Moving window correlation analyses at 10 and 20-year intervals generally show negative correlations between the two, with some exceptions, with Pearson's R ranging from −0.5 to +0.1. Periods of lower/higher P−E e.g. around 1900, 1915, 1962, and between ~1975–1990 CE, appear to correspond with increases in $\delta^{18}O_{ostracod}$ (Fig. 8), as well as periods of increased rainfall and reduced evaporation between ~1900–1920 CE and between ~1940–1960 CE, correspond with lower $\delta^{18}O_{ostracod}$. However, this is not always the case, for example between ~1920–1940 CE and in particular the period after ~2000 CE when no relationship is observed. It is possible that periods of poor correlation relate to changes in sedimentation rate not captured by the chronology.

Following the nuclear weapons testing of the 1960s, recorded by a marked increase in Pu concentration in the Lashmars Lagoon sediment, the sediment chronology is modelled to be more precise. However, since the 1950s, Kangaroo Island saw widespread land clearance with approximately 53 % of the island's native vegetation removed and

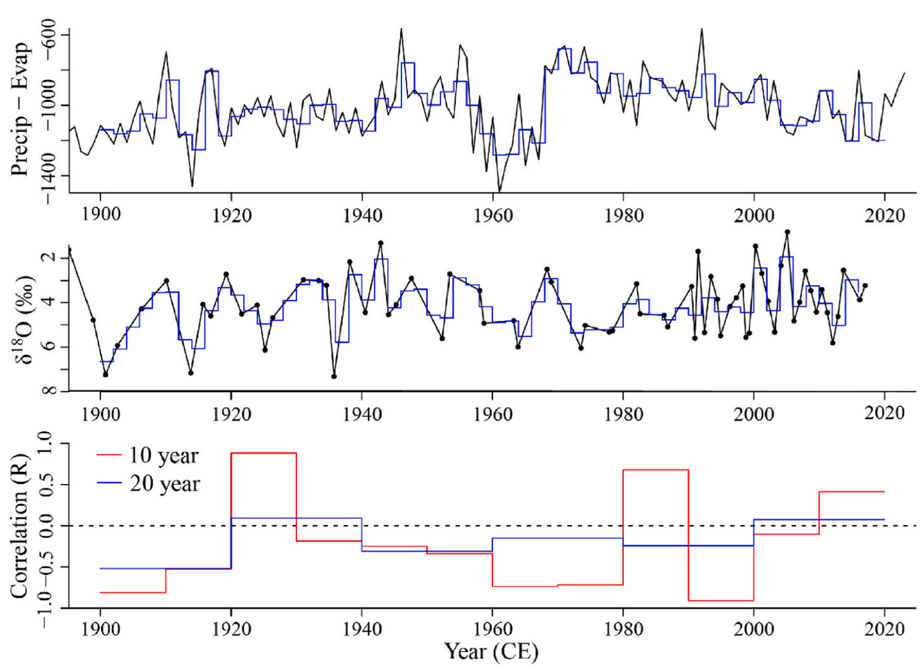

Fig. 8. Validation of $\delta^{18}O_{ostracod}$ as a hydroclimate proxy for Kangaroo Island, South Australia. Biannually binned (blue lines) precipitation–evaporation (P–E) data (upper figure) were compared with biannually binned $\delta^{18}O_{ostracod}$ values (middle figure) by testing for Pearson's correlation at 10 (bottom figure; red line) and 20 year (blue line) windows. (For interpretation of the references to colour in this figure legend, the reader is referred to the Web version of this article.)

converted to various agricultural grasslands and crops (Davies et al., 2002), which would have led to increased runoff, decreased water residence time and potentially an increase in sedimentation at Lashmars Lagoon, reducing the volume of the lake. These anthropogenic disturbances potentially explain the trend towards lower $\delta^{18}O_{ostracod}$ between ~1975–2005 CE, despite a corresponding decrease in effective moisture (Fig. 8). As a result, a comprehensive validation of $\delta^{18}O_{ostracod}$ as a proxy for effective moisture remains challenging but the generally negative correlation with P−E, as well as the extensive literature on lake isotope hydrology (Rex et al., 2024; Vystavna et al., 2020, 2021) and ostracod isotope geochemistry (De Deckker and Forester, 1988; Holmes and De Deckker, 2012; Ito et al., 2003) lead us to conclude that this is the primary driver for long term $\delta^{18}O_{ostracod}$ variability at Lashmars Lagoon.

4.4. Hydroclimatic variability over the last 2000 years

Our $\delta^{18}O_{ostracod}$ record enables the identification of several multi-decadal to centennial-scale dry and wet periods through the last ~2000 years. A total of four dry and four wet phases were determined from ~19 BCE – 1250 CE followed by the data gap from ~1250 to 1590 CE, then again a dry period from ~1590 to 1800 CE, and lastly a variable hydroclimate from ~1800 CE to the present (Fig. 9a). At the beginning of the Common Era, a dry period occurred up to around 140 CE followed by a prolonged wet period up to ~460 CE. *A. worooa*, an ostracod species which lives in predominantly freshwater environments, was found in samples from ~140 to 460 CE, supporting the inferred wet period based on lower $\delta^{18}O_{ostracod}$ values. Relatively wet periods are inferred for ~600–750 CE, ~870–950 CE, and ~1060–1250 CE. In the intervening periods, higher $\delta^{18}O_{ostracod}$ suggest relatively dry climates from ~460 to 600 CE, ~750–870 CE, and ~950–1060 CE. The overall duration of wet

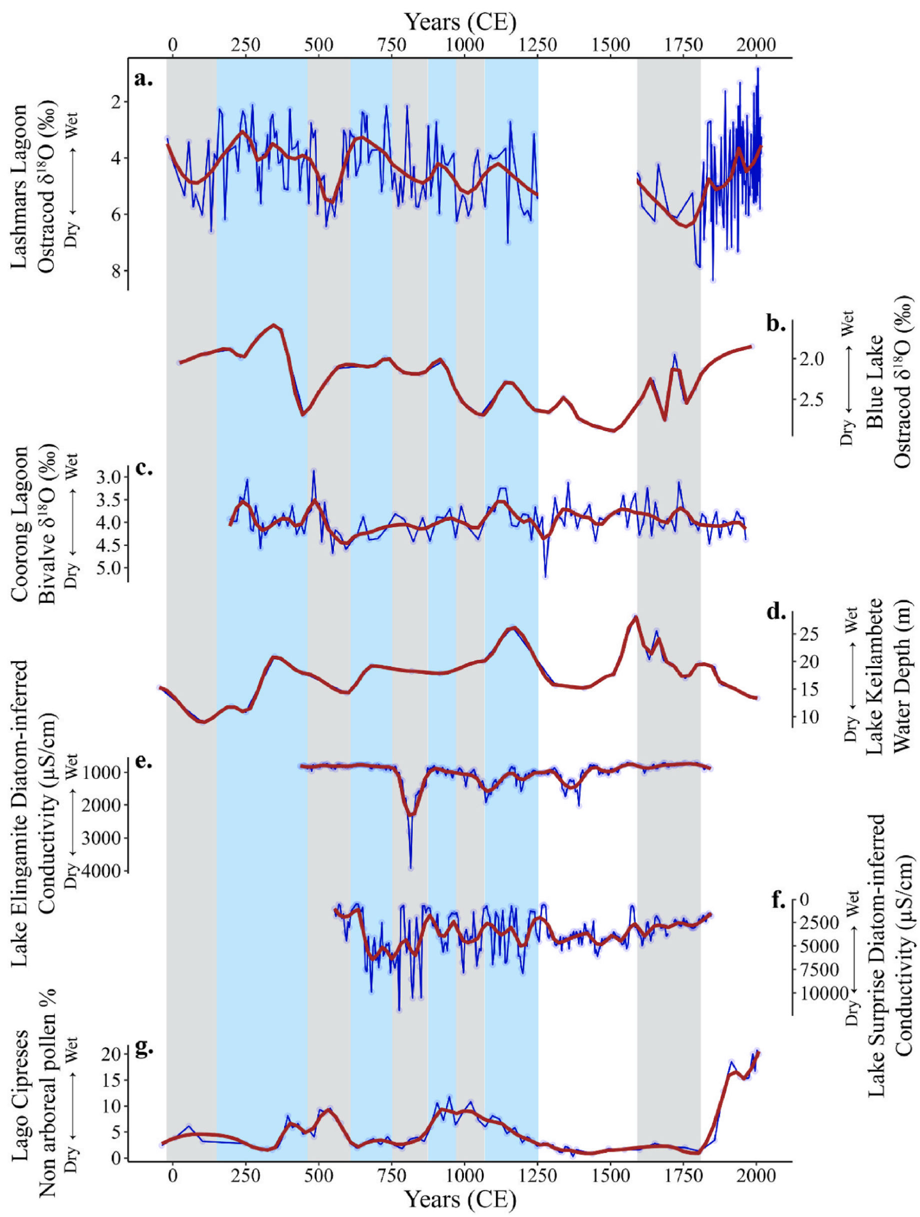

Fig. 9. a. Comparison of the $\delta^{18}O_{ostracod}$ record from Lashmars Lagoon with other records from south-eastern Australia, namely (b) ostracod $\delta^{18}O$ data from Blue Lake, Mt. Gambier, South Australia (Gouramanis et al., 2010); (c) bivalve $\delta^{18}O$ data from site C18, Coorong Lagoon, South Australia (Chamberlayne et al., 2023); (d) Grain size inferred lake water depth at Lake Keilambete, Victoria (Wilkins et al., 2013); diatom inferred lake water conductivity (salinity) from (e) Lake Elingamite; (f) and Lake Surprise, Victoria (Barr et al., 2014) and (g) Lago Cipreses non arboreal pollen concentration – interpreted to record changes in the southern westerly winds (Moreno et al., 2014). (For interpretation of the references to colour in this figure legend, the reader is referred to the Web version of this article.)

periods was found to be relatively longer (~750 years) than the dry periods (~500 years), and as a result, it can be concluded that the first millennium of the Common Era was relatively wet in the region.

The Lashmars Lagoon $\delta^{18}O_{ostracod}$ record exhibits some similarities to other hydroclimate records from south-eastern Australia, despite the limited age control of previous studies. In particular, the closest comparable study – based on oxygen isotope analyses of the ostracod *G. australica* in the sediments of Blue Lake, Mt. Gambier, South Australia (Gouramanis et al., 2010) exhibits a similar pattern of hydrological variation to Lashmars Lagoon (Fig. 9b). Interpretation of $\delta^{18}O$ at Blue Lake is complicated by the marked influence of groundwater throughflow, however isotope variability in lake water is ultimately tied to changes in regional precipitation and evaporation (Herczeg et al., 2003). By contrast, $\delta^{18}O$ analyses of the valves of the bivalve mollusc *Arthritica helmsi* in the sediments of the Coorong Lagoon, South Australia (Chamberlayne et al., 2023) only partially corresponds (wet periods ~195–275 CE, ~1060–1200 CE and dry periods ~500–600 CE, ~750–870 CE, and ~950–1050 CE) with the current study (Fig. 9c). It should be noted that the sediment chronology for the Coorong sediments was based on radiocarbon dating of fossil bivalve valves, with a reservoir age correction of ~600 years (Chamberlayne et al., 2023). Changes in the reservoir age of Coorong waters, e.g. due to changes in fluvial or marine or groundwater mixing in that dynamic estuarine lagoon, could therefore impart substantial alterations to the determined ages of the multi-decadal wet/dry events (Chamberlayne et al., 2023).

The lake level reconstruction from Lake Keilambete, Victoria, is arguably the most iconic record of hydroclimate variability in southern Australia (Wilkins et al., 2013), however, the comparison with Lashmars Lagoon $\delta^{18}O$ for the last ~2000 years does not reveal clear similarities (Fig. 9d). Lakes Surprise and Elingamite in Victoria both offer sub-decadal records of hydroclimate variability, via diatom-inferred salinity (Barr et al., 2014). While these records also do not consistently align with the Lashmars Lagoon $\delta^{18}O_{ostracod}$ record, they both exhibit three clear multi-decadal periods of higher salinity (lower effective moisture), which is similar to those inferred from this study, albeit offset in time. Of note, the present study infers that a wetter climate persisted between ~600 and 750 CE and that a drier climate occurred between ~750 and 870 CE. These wetter and drier periods largely align with the periods of low and high lake water salinity identified by Barr et al. (2014) (Fig. 9e and f). Pluvial conditions have been determined from Lake Callabonna in central southern Australia between 1050 ± 70 and 1100 ± 60 CE (Cohen et al., 2012) and clearly resemble the wet period of the current study.

The results presented here suggest that within these four identified dry periods, possible megadroughts (persistent, multi-year droughts (Cook et al., 2022)) occurred on Kangaroo Island from ~525 to 575 CE, ~770–790 CE, ~825–850 CE, and ~980–1020 CE. This does not preclude the presence of shorter droughts or droughts where ostracods are absent from the record. Vance et al. (2015) identified eight megadroughts using chloride from sea-salt in an ice core from Law Dome (East Antarctica) as a proxy for westerly wind activity, putatively linked to precipitation in Australia, including one 39-year drought over eastern Australia (1174–1212 CE). These droughts occurred between 1102 and 1212 CE. This finding is not supported by the findings at Lashmars Lagoon, as well as the studies conducted by Chamberlayne et al. (2023); Gouramanis et al. (2010); and Wilkins et al. (2013). The difference between the dry period we identified in this study and the eight megadroughts identified by Vance et al. (2015) is around 100 years. Given the inherent uncertainty of dating and age calibration, it is possible that these two separate dry periods are actually the same megadrought event.

Due to the absence of ostracods from ~1250 to 1590 CE, no hydroclimatic variability could be established for this time period. Following the gap in data, the $\delta^{18}O_{ostracod}$ record from Lashmars Lagoon suggests a possible trend towards drier conditions between ~1590 and 1800 CE, albeit poorly resolved, followed by a clear trend towards lower $\delta^{18}O_{ostracod}$ from ~1800 CE to the present, suggesting an increase in effective moisture. The post-1800 CE sediments also conatin abundant *A. worooa* and *C. novaezelandiae*, which suggest a predominantly freshwater environment, supporting our interpretation of the $\delta^{18}O_{ostracod}$ data. This trend is very similar to the ostracod $\delta^{18}O$ record from Blue Lake (Gouramanis et al., 2010), yet the trend is not observed in the Coorong Lagoon $\delta^{18}O$ data (Chamberlayne et al., 2023) and the opposite trend is inferred from Lake Keilambete grain size data (Wilkins et al., 2013). The Lake Elingamite and Lake Surprise diatom inferred conductivity data suggest a trend towards increased effective moisture into the mid-1800s (Barr et al., 2014; Tibby et al., 2018), although the interpretation of climate change from diatoms and lake water salinity following European colonisation is confounded by the impact of land clearance and agriculture (Barr et al., 2014). Further afield, the pigment-inferred precipitation record from Rebecca Lagoon, north-west Tasmania (Saunders et al., 2012) also suggest wetter climate during the 19th century. However, some records for south-eastern Australia, including the recorded decline in lake levels since colonisation, suggest a trend towards declining effective moisture since ~1900 CE (Tibby et al., 2018). This drying is opposite to the trend observed in the Lashmars Lagoon $\delta^{18}O_{ostracod}$ and other sediment records which suggests wetter conditions in the recent past. These differences may relate to the impact of intensified land use and land clearance on local hydrology, or alternatively to inter-regional differences in climate trends.

4.5. Drivers of regional hydroclimate in Kangaroo Island and south Australia

Australia's hydroclimate is driven by several major ocean-atmospheric interactions, including ENSO, IOD, SAM, and the IPO. These climatic drivers impact rainfall patterns across spring, autumn, and summer, operating on varying timescales (Cai et al., 2011; Gallant et al., 2012; Risbey et al., 2009; Vance et al., 2015). These drivers are not independent, but rather highly correlated (Risbey et al., 2009). Though South Australian rainfall is predominantly controlled by the SAM, ENSO and the IOD also act to reinforce dry or wet conditions in the region (Evans et al., 2009). Duxbury et al. (2024) suggested that the Leeuwin Current, which brings warm tropical waters to southern Australia and is teleconnected with ENSO, influences rainfall on Kangaroo Island. Van Ommen and Morgan (2010) identified an inverse precipitation relationship between Law Dome, East Antarctica, and south-western Western Australia (SWWA), linked by large-scale meridional atmospheric flow south of Australia, highlighting the strong influence of the SAM on SWWA rainfall. Over the last century, rainfall at the Cape Willoughby weather station, eastern Kangaroo Island, exhibits significant correlations with rainfall data from Perth (Western Australia) ($R^2 = 0.95$), Hobart (Tasmania) ($R^2 = 0.95$), and Melbourne (Caulfield, Victoria) ($R^2 = 0.95$) testifying to the prominent role of the Southern Westerly Winds (SWW) upon winter-dominant rainfall across the southern seaboard of Australia. The Southern Annular Mode (SAM) relates to the position and strength of the SWW, yet few high-quality reconstructions of the SAM exist which span the last ~2000 years. Moreno et al. (2014) used the deposition of non-arboreal pollen (NAP) in the sediments of Lago Cipreses, Patagonia, to reconstruct Holocene SAM variability. Similarly, Fletcher et al. (2018) inferred SAM variability using pollen from Lake Vera, Tasmania. Both the Lago Cipreses and Lake Vera records suggest two relatively brief but prominent periods of positive SAM centred around ~500 CE and ~1000 CE. Positive SAM is typically associated with drier climates in southern Australia, and these episodes roughly correspond with the periods of reduced effective moisture inferred from $\delta^{18}O_{ostracod}$ at Lashmars Lagoon, as well as other records in south-eastern Australia. The Lago Cipreses record also has a smaller peak in NAP at ~50 CE, which also corresponds with a period of reduced effective moisture at Lashmars Lagoon (Fig. 9g). However, this comparison is contradicted by the inferred shift towards positive SAM after ~1900 CE, which corresponds with $\delta^{18}O_{ostracod}$ evidence for wetter climate at

Lashmars Lagoon. This contradiction may relate to the aforementioned influence of post-colonial land clearance on the hydrology of Lashmars Lagoon, as well as similar effects upon the groundwater hydrology of Blue Lake, Mt. Gambier (Herczeg et al., 2003). However, it may also relate to inconsistencies in SAM reconstructions for the last millennium. Several studies have reconstructed the SAM index in detail for the last 1000 years using annually resolved ice core, coral, and tree ring records (Abram et al., 2014; Dätwyler et al., 2018; Villalba et al., 2012). Of note, these reconstructions suggest a shift towards positive SAM after ~1800 CE, i.e. earlier than that inferred from Lago Cipreses, and potentially corresponding with the drier conditions inferred from Lashmars Lagoon between ~1750 and 1800 CE (Fig. 9g). We therefore conclude that while further evidence is required to fully reconcile the drivers of hydroclimate variability in southern Australia, a dominant influence of the SWW is likely, as described by prominent, multi-decadal to centennial-scale oscillations changes in the Southern Annular Mode.

5. Conclusions

We have presented an ostracod-based oxygen isotope record for the past ~2000 years from the sediments of Lashmars Lagoon, Kangaroo Island. Validation of this record in comparison with instrumental climate data through the last century supports the interpretation that $\delta^{18}O_{ostracod}$ at Lashmars Lagoon exhibits a negative relationship with hydrological precipitation vs evaporation. Variations in $\delta^{18}O_{ostracod}$ values primarily reflect past hydroclimate, being driven by changes in the balance of rainfall and evaporation amount. However, complexities in our proxy-instrumental comparison highlight the need for further such studies in Australia. On the basis of $\delta^{18}O_{ostracod}$ data, significant dry events occurred around ~525–575 CE, ~770–790 CE, ~825–850 CE, and ~980–1020 CE, superimposed by several decadal-scale episodes of wetter/drier climate. Though the current study revealed a period of relatively dry climate between ~1590 and 1800 CE, this contrasts with several studies, which were interpreted to reflect wetter climates in south-eastern Australia. Comparison with reconstructed indices for major ocean–atmospheric interactions suggests that periods of drier climate on Kangaroo Island coincided with periods of positive Southern Annular Mode, reflecting the southwards shift of the southern westerly winds and a reduction in winter rainfall in southern Australia.

CrediT author statement

Mahfuzur Rahman: Conceptualization, Laboratory analyses, Formal analysis, Writing – original draft, Visualization. **Lucinda Duxbury:** Fieldwork, Laboratory analyses, Writing – review & editing. **Haidee Cadd:** Laboratory analyses, Writing – review & editing. **Robert Klaebe:** Laboratory analyses, Writing – review & editing. **Geraldine Jacobsen:** Laboratory analyses, Writing – review & editing. **John Tibby:** Conceptualization, Writing – review & editing. **Jonathan Tyler:** Conceptualization, Fieldwork, Formal analysis, Writing – review & editing, Funding acquisition.

Declaration of competing interest

The authors declare that they have no known competing financial interests or personal relationships that could have appeared to influence the work reported in this paper.

Acknowledgements

Amelia Orchard and Lucy Stokes are thanked for their preliminary analyses of ostracod oxygen isotopes from Lashmars Lagoon, although those data were not included in this manuscript. Kym Edwards is thanked for her help with sample preparation, and Boone Law for his ongoing help with fieldwork and mapping on Kangaroo Island. This project was supported by the ARC Centre of Excellence for Australian Biodiversity and Heritage (CABAH) and ARC Discovery Project DP190102782. Jonathan Tyler is funded by ARC Future Fellowship FT230100648. Radiocarbon dating at the Centre for Accelerator Science, ANSTO was funded by an ANSTO grant AP17752. We acknowledge the financial support from the Australian Government for the Centre for Accelerator Science at ANSTO through the National Collaborative Research Infrastructure Strategy (NCRIS). This research was developed and conducted on the lands of the Kaurna people, at The University of Adelaide. We further acknowledge that Karti/Karta (Kangaroo Island) is a place of deep cultural and spiritual significance for Aboriginal people in South Australia.

Appendix A. Supplementary data

Supplementary data to this article can be found online at https://doi.org/10.1016/j.quascirev.2025.109443.

Data availability

All data and/or code is contained within the submission.

References

Abram, N.J., Mulvaney, R., Vimeux, F., Phipps, S.J., Turner, J., England, M.H., 2014. Evolution of the southern annular mode during the past millennium. Nat. Clim. Change 4, 564–569.
Anadón, P., Utrilla, R., Vázquez, A., 2002. Mineralogy and Sr–Mg geochemistry of charophyte carbonates: a new tool for paleolimnological research. Earth Planet Sci. Lett. 197, 205–214.
Ankor, M.J., 2020. Hydrologic and Isotopic Lake Modelling for Palaeoclimate Research (Doctoral Dissertation). University of Adelaide.
Aquino-López, M.A., Blaauw, M., Christen, J.A., Sanderson, N.K., 2018. Bayesian analysis of 210 Pb dating. J. Agric. Biol. Environ. Stat. 23, 317–333.
Arvidson, R.S., Morse, J.W., 2014. 9.3 - formation and diagenesis of carbonate sediments. In: Holland, H.D., Turekian, K.K. (Eds.), Treatise on Geochemistry, second ed. Elsevier, Oxford, pp. 61–101.
Australia, E., 2001. A Directory of Important Wetlands in Australia, third ed. Environment Australia, Canberra.
Barr, C., Tibby, J., Gell, P., Tyler, J., Zawadzki, A., Jacobsen, G.E., 2014. Climate variability in south-eastern Australia over the last 1500 years inferred from the high-resolution diatom records of two crater lakes. Quat. Sci. Rev. 95, 115–131.
Beck, W.C., Grossman, E.L., Morse, J.W., 2005. Experimental studies of oxygen isotope fractionation in the carbonic acid system at 15, 25, and 40 C. Geochem. Cosmochim. Acta 69, 3493–3503.
Binskin, M., Bennett, A., Macintosh, A., 2020. Royal commission into national natural disaster arrangements report. Canberra Commonw. Aust. 56.
Blaauw, M., Christen, J.A., 2011. Flexible paleoclimate age-depth models using an autoregressive gamma process. Bayesian Analysis 6 (3), 457–474.
Bureau of Meteorology, 2023. Climate data online. Commonwealth of Australia, Bureau of Meteorology, Melbourne. Available from: http://www.bom.gov.au/jsp/ncc/cdio/weatherData/av?p_nccObsCode=139&p_display_type=dataFile&p_stn_num=022803.
Cadd, H., Sherborne-Higgins, B., Becerra-Valdivia, L., Tibby, J., Barr, C., Forbes, M., Cohen, T.J., Tyler, J., Vandergoes, M., Francke, A., 2022. The application of pollen radiocarbon dating and bayesian age-depth modeling for developing robust geochronological frameworks of wetland archives. Radiocarbon 64, 213–235.
Cai, W., Cowan, T., 2006. SAM and regional rainfall in IPCC AR4 models: can anthropogenic forcing account for southwest Western Australian winter rainfall reduction? Geophys. Res. Lett. 33.
Cai, W., Van Rensch, P., Cowan, T., Sullivan, A., 2010. Asymmetry in ENSO teleconnection with regional rainfall, its multidecadal variability, and impact. J. Clim. 23, 4944–4955.
Cai, W., van Rensch, P., Cowan, T., 2011. Influence of global-scale variability on the subtropical ridge over southeast Australia. J. Clim. 24 (1), 6035–6053. https://doi.org/10.1175/2011JCLI4149.
Carignan, R., Nriagu, J.O., 1985. Trace metal deposition and mobility in the sediments of two lakes near Sudbury, Ontario. Geochem. Cosmochim. Acta 49, 1753–1764.
Chamberlayne, B.K., Tyler, J.J., Haynes, D., Shao, Y., Tibby, J., Gillanders, B.M., 2023. Hydrological change in southern Australia over 1750 years: a bivalve oxygen isotope record from the Coorong Lagoon. Clim. Past 19, 1383–1396.
Clark, R.L., 1976. Vegetation History and the Influence of the Sea at Lashmar's Lagoon, Kangaroo Island, South Australia, 3,000 BP to the Present Day. Monash University, 1976.
Clark, R.L., 1983. Fire History from Fossil Charcoal in Lake and Swamp Sediments. The Australian National University, Australia.
Cleveland, W.S., Grosse, E., Shyu, W.M., 2017. Local regression models. In: Statistical Models in S. Routledge, pp. 309–376.
Cook, B.I., Palmer, J.G., Cook, E.R., Turney, C.S.M., Allen, K., Fenwick, P., O'Donnell, A., Lough, J.M., Grierson, P.F., Ho, M., 2016. The paleoclimate context and future

trajectory of extreme summer hydroclimate in eastern Australia. J. Geophys. Res. Atmos. 121, 12–820.
Cook, B.I., Smerdon, J.E., Cook, E.R., Williams, A.P., Anchukaitis, K.J., Mankin, J.S., Allen, K., Andreu-Hayles, L., Ault, T.R., Belmecheri, S., 2022. Megadroughts in the Common Era and the anthropocene. Nat. Rev. Earth Environ. 3, 741–757.
CSIRO and Bureau of Meteorology, 2015. Climate change in Australia information for Australia's natural resource management regions: Technical report. Available from: https://www.climatechangeinaustralia.gov.au/media/ccia/2.1.6/cms_page_media/168/CCIA_2015_NRM_TechnicalReport_WEB.pdf.
Dansgaard, W., 1964. Stable isotopes in precipitation. Tellus 16, 436–468.
Dätwyler, C., Neukom, R., Abram, N.J., Gallant, A.J.E., Grosjean, M., Jacques-Coper, M., Karoly, D.J., Villalba, R., 2018. Teleconnection stationarity, variability and trends of the Southern Annular Mode (SAM) during the last millennium. Clim. Dyn. 51, 2321–2339.
Davies, M., Twidale, C.R., Tyler, M.J., 2002. Natural History of Kangaroo Island.R. Soc. South Aust, second ed. p-93.
De Deckker, P., 1981. Taxonomy, Ecology and Palaeoecology of Ostracods from Australian Inland Waters (Doctoral Dissertation). University of Adelaide.
De Deckker, P., 1983. Notes on the ecology and distribution of non-marine ostracods in Australia. Hydrobiologia (The Hague) 106, 223–234.
De Deckker, P., Forester, R.M., 1988. The use of ostracods to reconstruct continental palaeoenvironmental records. Ostracoda earth Sci 175–199.
Decrouy, L., Vennemann, T.W., Ariztegui, D., 2011. Controls on ostracod valve geochemistry: Part 2. Carbon and oxygen isotope compositions. Geochem. Cosmochim. Acta 75, 7380–7399.
Devanand, A., Falster, G.M., Gillett, Z.E., Hobeichi, S., Holgate, C.M., Jin, C., Mu, M., Parker, T., Rifai, S.W., Rome, K.S., 2024. Australia's Tinderbox Drought: an extreme natural event likely worsened by human-caused climate change. Sci. Adv. 10, eadj3460.
Devriendt, L.S., McGregor, H.V., Chivas, A.R., 2017. Ostracod calcite records the 18O/16O ratio of the bicarbonate and carbonate ions in water. Geochem. Cosmochim. Acta 214, 30–50.
Dey, R., Bador, M., Alexander, L.V., Lewis, S.C., 2021. The drivers of extreme rainfall event timing in Australia. Int. J. Climatol. 41, 6654–6673.
Dijk, Van, A.I, J.M., Beck, Hylke E., Crosbie, Russell S., De, Jeu, Richard, A.M., Liu, Yi Y., Podger, Geoff M., Timbal, Bertrand, Viney, Neil R., Dijk, V., Beck, H.E., Crosbie, R.S., De Jeu, R.A.M., Liu, Y.Y., Podger, G.M., Timbal, B., Viney, N.R., 2013. The Millennium Drought in southeast Australia (2001–2009): natural and human causes and implications for water resources, ecosystems, economy, and society. Water Resour. Res. 49, 1040–1057. https://doi.org/10.1002/WRCR.20123.
Dixon, B.C., 2019. Data synthesis and modern cave process studies in southeastern Australia: towards improving regional palaeoclimate records for the Common Era (Doctoral dissertation). University of Adelaide.
Dixon, B.C., Tyler, J.J., Lorrey, A.M., Goodwin, I.D., Gergis, J., Drysdale, R.N., 2017. Low-resolution Australasian palaeoclimate records of the last 2000 years. Clim. Past 13, 1403–1433.
Dougherty, A.J., 2018. Punctuated transgression (?): comment on Oliver, TSN. In: Donaldson, P., Sharples, C., Roach, M., Woodroffe, C.D. (Eds.), Punctuated progradation of the Seven Mile Beach Holocene barrier system, southeastern Tasmania, Mar. Geol., vol. 405, pp. 120–130.
Duxbury, L., 2022. Holocene climate, fire and ecosystem change on Kangaroo Island, South Australia (Master of Philosophy Dissertation). University of Adelaide.
Duxbury, L.C., Johns-Mead, L.Y., Cadd, H., Francke, A., Löhr, S.C., Law, W.B., Armbrecht, L., Hall, P.A., Zawadzki, A., Jacobsen, G.E., 2024. Holocene climate and catchment change inferred from the geochemistry of Lashmars Lagoon, Kangaroo Island (Karti/Karta), southern Australia. Palaeogeogr. Palaeoclimatol. Palaeoecol. 634, 111928.
Evans, A.D., Bennett, J.M., Ewenz, C.M., 2009. South Australian rainfall variability and climate extremes. Clim. Dyn. 33, 477–493. https://doi.org/10.1007/S00382-008-0461-Z.
Fischer, M.J., Treble, P.C., 2008. Calibrating climate-δ18O regression models for the interpretation of high-resolution speleothem δ18O time series. J. Geophys. Res. Atmos. 113.
Francke, A., Conze, R., Pierdominici, S., Gorgas, T., 2017. Core correlation using Corelyzer, Corelator and the drilling information system. Planning, Manag. Exec. Cont. Sci. Drill. Proj. 93–101.
Gallant, A.J.E., Kiem, A.S., Verdon-Kidd, D.C., Stone, R.C., Karoly, D.J., 2012. Hydrology and earth system Sciences understanding hydroclimate processes in the murray-darling basin for natural resources management. Hydrol. Earth Syst. Sci. 16, 2049–2068. https://doi.org/10.5194/hess-16-2049-2012.
Gallant, A.J.E., Phipps, S.J., Karoly, D.J., Mullan, A.B., Lorrey, A.M., 2013. Nonstationary Australasian teleconnections and implications for paleoclimate reconstructions. J. Clim. 26, 8827–8849.
García, A., 1987. El gametangio femenino de charophyta actuales de Argentina comparado con el registro fósil correspondiente (Doctoral dissertation). Universidad Nacional de La Plata.
Goodwin, I.D., Browning, S., Lorrey, A.M., Mayewski, P.A., Phipps, S.J., Bertler, N.A.N., Edwards, R.P., Cohen, T.J., van Ommen, T., Curran, M., 2014. A reconstruction of extratropical Indo-Pacific sea-level pressure patterns during the Medieval Climate Anomaly. Clim. Dyn. 43, 1197–1219.
Gouramanis, C., Wilkins, D., De Deckker, P., 2010. 6000 years of environmental changes recorded in Blue Lake, South Australia, based on ostracod ecology and valve chemistry. Palaeogeogr. Palaeoclimatol. Palaeoecol. 297, 223–237.
Gouramanis, C., Dodson, J., Wilkins, D., De Deckker, P., Chase, B.M., 2012. Holocene palaeoclimate and sea level fluctuation recorded from the coastal Barker Swamp, Rottnest Island, south-western Western Australia. Quat. Sci. Rev. 54, 40–57.
Gouramanis, C., De Deckker, P., Switzer, A.D., Wilkins, D., 2013. Cross-continent comparison of high-resolution Holocene climate records from southern Australia - deciphering the impacts of far-field teleconnections. Earth-Science Rev. 121, 55–72. https://doi.org/10.1016/J.EARSCIREV.2013.02.006.
Granath, G., Evans, C.D., Strengbom, J., Fölster, J., Grelle, A., Strömqvist, J., Köhler, S.J., 2021. The impact of wildfire on biogeochemical fluxes and water quality in boreal catchments. Biogeosciences 18, 3243–3261.
Hendon, H.H., Thompson, D.W.J., Wheeler, M.C., 2007. Australian rainfall and surface temperature variations associated with the Southern Hemisphere annular mode. J. Clim. 20, 2452–2467.
Herbst, A., von Tümpling, W., Schubert, H., 2018. The seasonal effects on the encrustation of charophytes in two hard-water lakes. J. Phycol. 54, 630–637.
Herczeg, A.L., Leaney, F.W., Dighton, J.C., Lamontagne, S., Schiff, S.L., Telfer, A.L., English, M.C., 2003. A modern isotope record of changes in water and carbon budgets in a groundwater-fed lake: blue Lake, South Australia. Limnol. Oceanogr. 48, 2093–2105.
Hogg, A.G., Heaton, T.J., Hua, Q., Palmer, J.G., Turney, C.S.M., Southon, J., Bayliss, A., Blackwell, P.G., Boswijk, G., Ramsey, C.B., 2020. SHCal20 Southern Hemisphere calibration, 0–55,000 years cal BP. Radiocarbon 62, 759–778.
Holmes, J.A., De Deckker, P., 2012. The chemical composition of ostracod shells: applications in Quaternary palaeoclimatology. In: Developments in Quaternary Sciences. Elsevier, pp. 131–143.
Holmes, J., Burn, M., Cisneros-Dozal, L.M., Jones, M., Metcalfe, S., 2023. An 1800-year oxygen-isotope record of short-and long-term hydroclimate variability in the northern neotropics from a Jamaican marl lake. Quat. Sci. Rev. 301, 107930.
Hua, Q., Jacobsen, G.E., Zoppi, U., Lawson, E.M., Williams, A.A., Smith, A.M., McGann, M.J., 2001. Progress in radiocarbon target preparation at the ANTARES AMS Centre. Radiocarbon 43, 275–282.
Hughes, L., 2003. Climate change and Australia: trends, projections and impacts. Austral Ecol. 28, 423–443.
Ito, E., De Deckker, P., Eggins, S.M., 2003. Ostracodes and their shell chemistry: implications for paleohydrologic and paleoclimatologic applications. Paleontol. Socio. Pap. 9, 119–152.
Kiem, A.S., Austin, E.K., 2013. Drought and the future of rural communities: opportunities and challenges for climate change adaptation in regional Victoria, Australia. Glob. Environ. Change 23, 1307–1316. https://doi.org/10.1016/J.GLOENVCHA.2013.06.003.
Kiem, A.S., Franks, S.W., 2004. Multi-decadal variability of drought risk, eastern Australia. Hydrol. Process. 18, 2039–2050.
Kiem, A.S., Johnson, F., Westra, S., Van Dijk, A., Evans, J.P., O'donnell, A., Rouillard, A., Barr, C., Tyler, J., Thyer, M., Jakob, D., Woldemeskel, F., Bellie, Sivakumar, Mehrotra, R., 2016. Natural hazards in Australia: droughts. Clim. Change 139, 37–54. https://doi.org/10.1007/s10584-016-1798-7.
Kim, S.-T., O'Neil, J.R., 1997. Equilibrium and nonequilibrium oxygen isotope effects in synthetic carbonates. Geochem. Cosmochim. Acta 61, 3461–3475.
Koinig, K.A., Shotyk, W., Lotter, A.F., Ohlendorf, C., Sturm, M., 2003. 9000 years of geochemical evolution of lithogenic major and trace elements in the sediment of an alpine lake–the role of climate, vegetation, and land-use history. J. Paleolimnol. 30, 307–320.
Kufel, L., Strzałek, M., Biardzka, E., 2016. Site-and species-specific contribution of charophytes to calcium and phosphorus cycling in lakes. Hydrobiologia (The Hague) 767, 185–195.
Kurganskaya, I., Churakov, S.V., 2018. Carbonate dissolution mechanisms in the presence of electrolytes revealed by grand canonical and kinetic Monte Carlo Modeling. J. Phys. Chem. C 122, 29285–29297.
Lampert, R.J., 1981. The great Kartan mystery. Aust. Archaeol. 107–109.
Leblanc, M., Tweed, S., Van Dijk, A., Timbal, B., 2012. A review of historic and future hydrological changes in the Murray-Darling Basin. Global Planet. Change 80–81, 226–246. https://doi.org/10.1016/J.GLOPLACHA.2011.10.012.
Leitch, A.R., 1989. Formation and ultrastructure of a complex, multilayered wall around the oospore of *Chara* and *Lamprothamnium* (Characeae). Br. Phycol. J. 24, 229–236.
Li, X., Liu, W., 2010. Oxygen isotope fractionation in the ostracod Eucypris mareotica: results from a culture experiment and implications for paleoclimate reconstruction. J. Paleolimnol. 43, 111–120.
Li, X., Liu, W., Xu, L., 2012. Stable oxygen isotope of ostracods in recent sediments of Lake Gahai in the Qaidam Basin, northwest China: the implications for paleoclimatic reconstruction. Global Planet. Change 94, 13–19.
Liu, W., Li, X., Zhang, L., An, Z., Xu, L., 2009. Evaluation of oxygen isotopes in carbonate as an indicator of lake evolution in arid areas: the modern Qinghai Lake, Qinghai–Tibet Plateau. Chem. Geol. 268, 126–136.
McGowan, H.A., Marx, S.K., Denholm, J., Soderholm, J., Kamber, B.S., 2009. Reconstructing annual inflows to the headwater catchments of the murray river, Australia, using the pacific decadal oscillation. Geophys. Res. Lett. 36.
Moreno, P.I., Vilanova, I., Villa-Martínez, R., Garreaud, R.D., Rojas, M., De Pol-Holz, R., 2014. Southern Annular Mode-like changes in southwestern Patagonia at centennial timescales over the last three millennia. Nat. Commun. 5, 4375.
Murphy, B.F., Timbal, B., 2008. A review of recent climate variability and climate change in southeastern Australia. Int. J. Climatol. 28, 859–879. https://doi.org/10.1002/JOC.1627.
Nesbitt, W.A., Mucci, A., 2021. Direct evidence of sediment carbonate dissolution in response to bottom-water acidification in the Gulf of St. Lawrence, Canada. Can. J. Earth Sci. 58, 84–92.
Neukom, R., Gergis, J., 2012. Southern Hemisphere high-resolution palaeoclimate records of the last 2000 years. Holocene 22, 501–524.

Oliver, T.S.N., Donaldson, P., Sharples, C., Roach, M., Woodroffe, C.D., 2017. Punctuated progradation of the seven mile beach Holocene barrier system, southeastern Tasmania. Mar. Geol. 386, 76–87.

Oliver, T.S.N., Donaldson, P., Tamura, T., 2022. Embayment-scale coastal evolution and shoreline progradation in southeast Tasmania, Australia. Mar. Geol. 444, 106725.

Palmer, J.G., Verdon-Kidd, D., Allen, K.J., Higgins, P., Cook, B.I., Cook, E.R., Turney, C.S. M., Baker, P.J., 2023. Drought and deluge: the recurrence of hydroclimate extremes during the past 600 years in eastern Australia's Natural Resource Management (NRM) clusters. Nat. Hazards 1–23.

Parker, S.E., Harrison, S.P., Comas-Bru, L., Kaushal, N., LeGrande, A.N., Werner, M., 2021. A data–model approach to interpreting speleothem oxygen isotope records from monsoon regions. Clim. Past 17, 1119–1138.

Pashkova, G.V., Aisueva, T.S., Finkelshtein, A.L., Ivanov, E.V., Shchetnikov, A.A., 2016. Analytical approaches for determination of bromine in sediment core samples by X-ray fluorescence spectrometry. Talanta 160, 375–380.

Pérez, L., Curtis, J., Brenner, M., Hodell, D., Escobar, J., Lozano, S., Schwalb, A., 2013. Stable isotope values (δ18O & δ13C) of multiple ostracode species in a large Neotropical lake as indicators of past changes in hydrology. Quat. Sci. Rev. 66, 96–111.

Power, S., Casey, T., Folland, C., Colman, A., Mehta, V., 1999. Inter-decadal modulation of the impact of ENSO on Australia. Clim. Dyn. 15, 319–324.

Power, S., Haylock, M., Colman, R., Wang, X., 2006. The predictability of interdecadal changes in ENSO activity and ENSO teleconnections. J. Clim. 19, 4755–4771.

Quigley, M.C., Horton, T., Hellstrom, J.C., Cupper, M.L., Sandiford, M., 2010. Holocene climate change in arid Australia from speleothem and alluvial records. Holocene 20, 1093–1104.

Rahman, M., Chaplin, J., Pinder, A., 2023. The biology of giant ostracods (Crustacea, Cyprididae), a review focusing on the Mytilocypridinae from Australian inland waters. Mar. Freshw. Res. 74, 1–19.

Renberg, I., Hansson, H., 2008. The HTH sediment corer. J. Paleolimnol. 40, 655–659.

Rex, C.L., Tyler, J.J., Nagaya, K., Staff, R.A., Leng, M.J., Yamada, K., Kitaba, I., Kitagawa, J., Kojima, H., Nakagawa, T., 2024. The contemporary stable isotope hydrology of Lake Suigetsu and surrounding catchment (Japan) and its implications for sediment-derived palaeoclimate records. Quat. Sci. Adv. 13, 100145.

Risbey, J.S., Pook, M.J., McIntosh, P.C., Wheeler, M.C., Hendon, H.H., 2009. On the remote drivers of rainfall variability in Australia. Mon. Weather Rev. 137, 3233–3253.

Robinson, A.C., Armstrong, D.M., 1999. A biological survey of Kangaroo island South Australia, 1989 and 1990. Herit. Biodivers. Sect. Dep. Environ. Herit. Aborig. Aff., South Aust.. Available from: https://data.environment.sa.gov.au/Content/Publications/Kangaroo-Island-BioSurvey.pdf

Saunders, K.M., Taffs, K.H., 2009. Palaeoecology: a tool to improve the management of Australian estuaries. J. Environ. Manag. 90, 2730–2736.

Saunders, K.M., Kamenik, C., Hodgson, D.A., Hunziker, S., Siffert, L., Fischer, D., Fujak, M., Gibson, J.A.E., Grosjean, M., 2012. Late Holocene changes in precipitation in northwest Tasmania and their potential links to shifts in the Southern Hemisphere westerly winds. Global Planet. Change 92, 82–91.

Seki, A., Tada, R., Kurokawa, S., Murayama, M., 2019. High-resolution Quaternary record of marine organic carbon content in the hemipelagic sediments of the Japan Sea from bromine counts measured by XRF core scanner. Prog. Earth Planet. Sci. 6, 1–12.

Soulié-Märsche, I., García, A., 2015. Gyrogonites and oospores, complementary viewpoints to improve the study of the charophytes (Charales). Aquat. Bot. 120, 7–17.

Strzałek, M., Kufel, L., Apolinarska, K., Becher, M., Biardzka, E., Brzozowski, M., Kiełczewski, R., Kowalewski, G., Pukacz, A., Woszczyk, M., 2024. Recycling and deposition of inorganic carbon from calcium carbonate encrustations of charophytes. Limnol. Oceanogr. 69, 279–289.

Talbot, M.R., 1990. A review of the palaeohydrological interpretation of carbon and oxygen isotopic ratios in primary lacustrine carbonates. Chem. Geol. Isot. Geosci. Sect. 80, 261–279.

Taylor, R., 2008. Unearthed: the Aboriginal Tasmanians of Kangaroo Island. Wakefield Press.

Tozer, C.R., Vance, T.R., Roberts, J.L., Kiem, A.S., Curran, M.A.J., Moy, A.D., 2016. An ice core derived 1013-year catchment-scale annual rainfall reconstruction in subtropical eastern Australia. Hydrol. Earth Syst. Sci. 20, 1703–1717.

Treble, P.C., Budd, W.F., Hope, P.K., Rustomji, P.K., 2005. Synoptic-scale climate patterns associated with rainfall δ18O in southern Australia. J. Hydrol. 302, 270–282.

Tyler, J.J., Marshall, J.C., Schulz, C., Barr, C., Hofmann, H., Blessing, J.J., McCoy, K., McGregor, G.B., Tibby, J., 2022. Hydrological and isotopic variability of perched wetlands on north stradbroke island (Minjerribah), Australia: implications for understanding the effects of past and future climate change. Front. Environ. Sci. 10, 868114.

Van Ommen, T.D., Morgan, V., 2010. Snowfall increase in coastal East Antarctica linked with southwest Western Australian drought. Nat. Geosci. 3, 267–272.

Vance, T.R., van Ommen, T.D., Curran, M.A.J., Plummer, C.T., Moy, A.D., 2013. A millennial proxy record of ENSO and eastern Australian rainfall from the Law Dome ice core, East Antarctica. J. Clim. 26, 710–725.

Vance, T.R., Roberts, J.L., Plummer, C.T., Kiem, A.S., Van Ommen, T.D., 2015. Interdecadal Pacific variability and eastern Australian megadroughts over the last millennium. Geophys. Res. Lett. 42, 129–137.

Verdon-Kidd, D.C., Kiem, A.S., 2009. Nature and causes of protracted droughts in southeast Australia: comparison between the Federation, WWII, and Big Dry droughts. Geophys. Res. Lett. 36, 22707. https://doi.org/10.1029/2009GL041067.

Villalba, R., Lara, A., Masiokas, M.H., Urrutia, R., Luckman, B.H., Marshall, G.J., Mundo, I.A., Christie, D.A., Cook, E.R., Neukom, R., 2012. Unusual southern Hemisphere tree growth patterns induced by changes in the southern annular mode. Nat. Geosci. 5, 793–798.

Von Grafenstein, U., Erlernkeuser, H., Trimborn, P., 1999. Oxygen and carbon isotopes in modern fresh-water ostracod valves: assessing vital offsets and autecological effects of interest for palaeoclimate studies. Palaeogeogr. Palaeoclimatol. Palaeoecol. 148, 133–152.

Vystavna, Y., Schmidt, S.I., Kopáček, J., Hejzlar, J., Holko, L., Matiatos, I., Wassenaar, L. I., Persoiu, A., Badaluta, C.A., Huneau, F., 2020. Small-scale chemical and isotopic variability of hydrological pathways in a mountain lake catchment. J. Hydrol. 585, 124834.

Vystavna, Y., Harjung, A., Monteiro, L.R., Matiatos, I., Wassenaar, L.I., 2021. Stable isotopes in global lakes integrate catchment and climatic controls on evaporation. Nat. Commun. 12, 7224.

Walling, D.E., Meyers, R.A., 2012. Fallout radionuclides and the study of erosion and sedimentation. Encycl. Sustain. Sci. Technol. Springer 3705–3768.

Walshe, K., 2005. Indigenous archaeological sites and the black swamp fossil bed: rocky river precinct, flinders chase national park, Kangaroo island, South Australia. Aust. Archaeol. 60, 61–64.

Wilcken, K.M., Hotchkis, M., Levchenko, V., Fink, D., Hauser, T., Kitchen, R., 2015. From carbon to actinides: a new universal 1MV accelerator mass spectrometer at ANSTO. Nucl. Instruments Methods Phys. Res. Sect. B Beam Interact. with Mater. Atoms 361, 133–138.

Wilkins, D., Gouramanis, C., De Deckker, P., Fifield, L.K., Olley, J., 2013. Holocene lake-Level fluctuations in lakes Keilambete and gnotuk, southwestern Victoria, Australia. Holocene 23, 784–795.

Wittwer, G., Waschik, R., 2021. Estimating the economic impacts of the 2017–2019 drought and 2019–2020 bushfires on regional NSW and the rest of Australia. Aust. J. Agric. Resour. Econ. 65, 918–936.

Wright, H.E., 1967. A square-rod piston sampler for lake sediments. J. Sediment. Res. 37, 975–976.

Young, L.B., Harvey, H.H., 1992. Geochemistry of Mn and Fe in lake sediments in relation to lake acidity. Limnol. Oceanogr. 37, 603–613.